AD-A054 831 ARMAMENT DEVELOPMENT AND TEST CENTER EGLIN AFB FLA F/G 16/4
THREE DIMENSIONAL TRANSONIC MODEL TESTING ON A ROCKET SLED TRAC--ETC(U)
JAN 78 D J KRUPOVAGE

UNCLASSIFIED ADTC-TR-78-8 NL

| OF |
AD
A054831

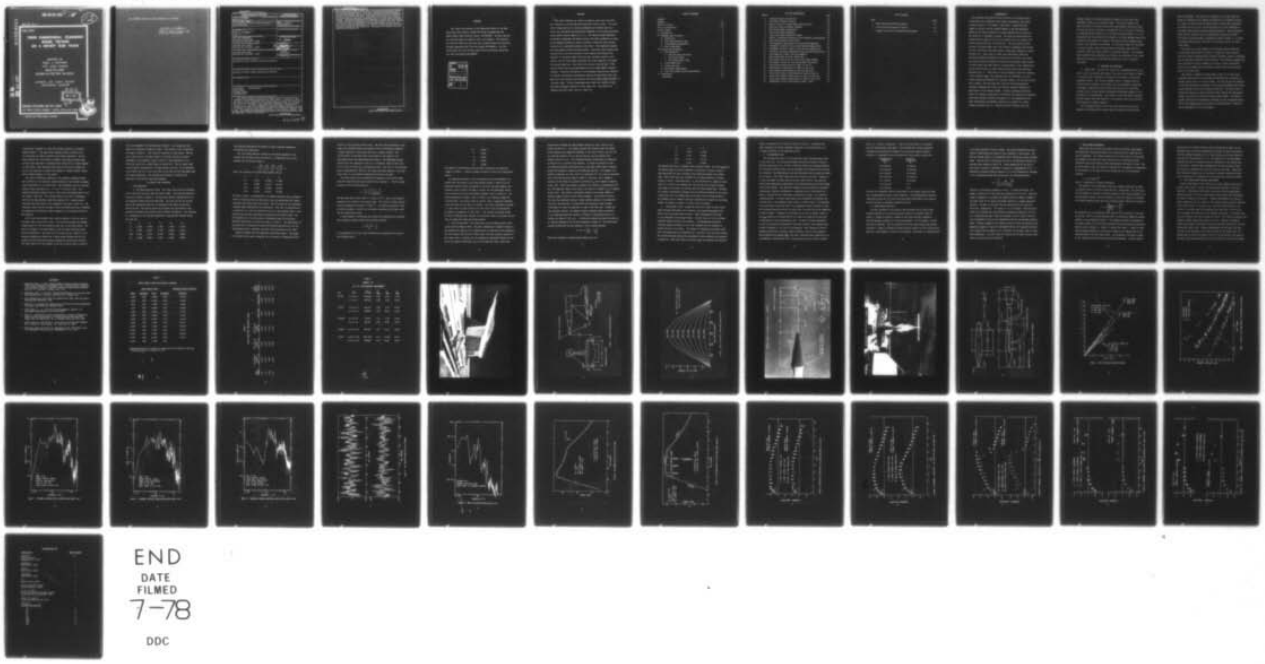

END
DATE
FILMED
7-78
DDC

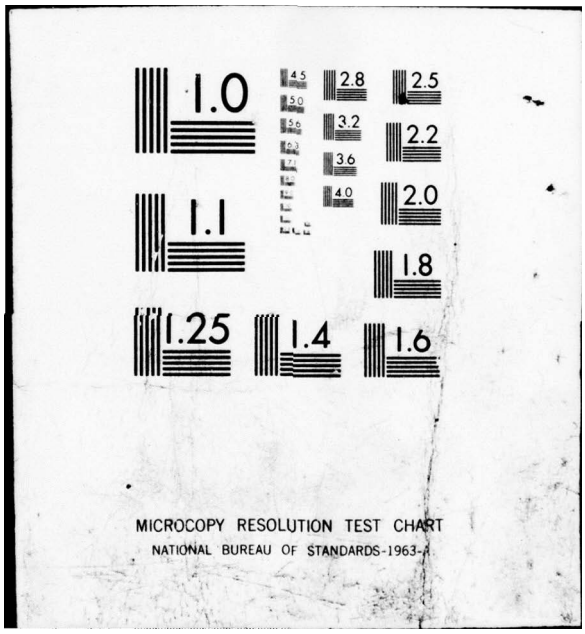
1.0
1.1
1.25
1.4
1.6
1.8
2.0
2.2
2.5
2.8
3.2
3.6
4.0
4.5
5.0
5.6
MICROCOPY RESOLUTION TEST CHART
NATIONAL BUREAU OF STANDARDS-1963-A

(12)

ADTC-TR-78-8

FINAL REPORT

THREE DIMENSIONAL TRANSONIC MODEL TESTING ON A ROCKET SLED TRACK

PREPARED BY
DANIEL J. KRUPOVAGE
TEST TRACK DIVISION
6585TH TEST GROUP
HOLLOMAN AIR FORCE BASE, NEW MEXICO

APPROVED FOR PUBLIC RELEASE
DISTRIBUTION UNLIMITED

ARMAMENT DEVELOPMENT AND TEST CENTER
AIR FORCE SYSTEMS COMMAND - UNITED STATES AIR FORCE
EGLIN AIR FORCE BASE, FLORIDA

THIS TECHNICAL REPORT HAS BEEN REVIEWED AND IS APPROVED.

Wallace B. Adam

WALLACE B. ADAM, Lt Colonel, USAF
Chief, Test Track Division

UNCLASSIFIED

SECURITY CLASSIFICATION OF THIS PAGE (When Data Entered)

REPORT DOCUMENTATION PAGE	READ INSTRUCTIONS BEFORE COMPLETING FORM
1. REPORT NUMBER (14) ADTC-TR-78-8	2. GOVT ACCESSION NO. / 3. RECIPIENT'S CATALOG NUMBER
4. TITLE (and Subtitle) (6) Three Dimensional Transonic Model Testing on a Rocket Sled Track.	5. TYPE OF REPORT & PERIOD COVERED (9) Final rept., / 6. PERFORMING ORG. REPORT NUMBER
7. AUTHOR(s) Daniel J. Krupovage (10)	8. CONTRACT OR GRANT NUMBER(s)
9. PERFORMING ORGANIZATION NAME AND ADDRESS 6585 Test Group (AFSC) Test Track Division (TK) Holloman AFB, New Mexico 88330	10. PROGRAM ELEMENT, PROJECT, TASK AREA & WORK UNIT NUMBERS JON: 99930000
11. CONTROLLING OFFICE NAME AND ADDRESS 6585 Test Group (AFSC) Holloman AFB, New Mexico 88330	12. REPORT DATE (11) Jan 78 / 13. NUMBER OF PAGES (12) 54p
14. MONITORING AGENCY NAME & ADDRESS (if different from Controlling Office) 6585 Test Group (AFSC) Holloman AFB, New Mexico 88330	15. SECURITY CLASS. (of this report) Unclassified / 15a. DECLASSIFICATION/DOWNGRADING SCHEDULE NA

16. DISTRIBUTION STATEMENT (of this Report)

Approved for public release; distribution unlimited.

17. DISTRIBUTION STATEMENT (of the abstract entered in Block 20, if different from Report)

Approved for public release; distribution unlimited

18. SUPPLEMENTARY NOTES

19. KEY WORDS (Continue on reverse side if necessary and identify by block number)

Rocket Sleds
Track Testing
Transonic Testing
Flow Angularity
Sled Vibration

20. ABSTRACT (Continue on reverse side if necessary and identify by block number)

This report presents the results of several rocket sled runs which were conducted on the Holloman High Speed Test Track facility. Objective of these runs was to collect aerodynamic and vibratory data on a rocket test sled which was specifically designed to test large three dimensional models at Mach numbers up to 1.5. The vehicle design emphasizes aerodynamic cleanliness and minimum frontal area while attempting to incorporate maximum stiffness in order to provide a relatively rigid testing platform in an undisturbed transonic flow field. Flow angularity measurements were made by three different methods. One

DD FORM 1 JAN 73 1473 EDITION OF 1 NOV 65 IS OBSOLETE

UNCLASSIFIED

SECURITY CLASSIFICATION OF THIS PAGE (When Data Entered)

404038 B

method used pressure data obtained from a five hole direction probe, another used pressure data measured on a wing-body model which had been previously tested in wind tunnels, and the third method determined flow field angularity from model sting strain gage data. Mach number was calculated in two ways: from electro-optical space-time measurements and also using dynamic pressure readings. Vibration information on the sled/model interface was collected by triaxial accelerometer measurements obtained during several sled runs. Model and sting dynamics were measured with strain gage bridges installed on the model sting. Pressure measurements were taken on a wing-body model which was originally designed for wind tunnel use. The results are compared with wind tunnel data up to Mach 0.9.

FOREWORD

This report was prepared in the Engineering Branch of the High Speed Test Track Facility, 6585th Test Group, Holloman AFB, New Mexico 88330, under Technical Support JON 99930000. The data reported was collected under two separate track test programs. The vibration and five hole direction probe data were collected under the Track Test Division Operations Plan 17Y-R and program JON 9950S014. The flow survey model data was collected under Track Test Division Operations Plan 9B-A and program JON AEDCSP01.

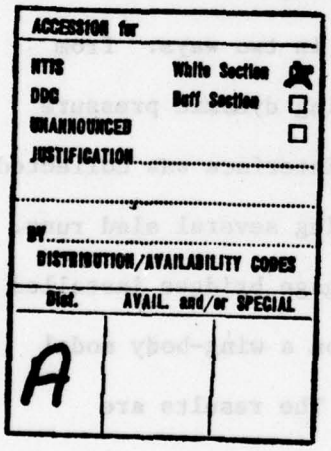

ABSTRACT

This report presents the results of several rocket sled runs which were conducted on the Holloman High Speed Test Track facility. The objective of these runs was to collect aerodynamic and vibratory data on a rocket test sled which was specifically designed to test large three dimensional models at Mach numbers up to 1.5. The vehicle design emphasizes aerodynamic cleanliness and minimum frontal area while attempting to incorporate maximum stiffness in order to provide a relatively rigid testing platform in an undisturbed transonic flow field. Flow angularity measurements were made by three different methods. One method used pressure data obtained from a five hole direction probe, another used pressure data measured on a wing-body model which had been previously tested in wind tunnels, and the third method determined flow field angularity from model sting strain gage data. Mach number was calculated in two ways: from electro-optical space-time measurements and also using dynamic pressure readings. Vibration information on the sled/model interface was collected by triaxial accelerometer measurements obtained during several sled runs. Model and sting dynamics were measured with strain gage bridges installed on the model sting. Pressure measurements were taken on a wing-body model which was originally designed for wind tunnel use. The results are compared with wind tunnel data up to Mach 0.9

TABLE OF CONTENTS

Foreword	i
Abstract	ii
Table of Contents	iii
List of Illustrations	iv
List of Tables	v
I. Introduction	1
II. Equipment and Procedures	2
A. Rocket Sled	2
B. Five Hole Direction Probe	4
C. Accelerometer Installation	5
D. Flow Survey Model	5
III. Results and Discussion	7
A. Flow Angularity	7
1. Five Hole Direction Probe	7
2. Flow Survey Model	10
3. Flow Survey Model Sting	12
B. Accelerometer Data	13
C. Strain Gage Data	14
D. Mach Number Measurements	15
E. Flow Survey Model Pressure Measurements	17
IV. Conclusions	19
References	20

LIST OF ILLUSTRATIONS

Figure		Page
1	Transonic Rocket Sled FDN 7314	24
2	Sled Model Interface Location	25
3	Angle of Yaw Due to Winds Versus Wind Direction	26
4	Direction Probe and Support Assembly	27
5	Flow Survey Model Installation	28
6	Flow Survey Model Dimensions	29
7	Sting Strain Gage Calibration Values	30
8	Effects of Digitizing Process on Flow Angularity Calculations	31
9	Center Body Pressure Coefficients	32
10	Flow Angularity Determined from Sting Strain Gage Data	33
11	Sled/Model Interface Vertical Power Spectral Density Plot	34
12	Sled/Model Interface Lateral Power Spectral Density Plot	35
13	Sled/Model Interface Longitudinal Power Spectral Density Plot	36
14	Data Sampling of Model and Sting Dynamics	37
15	Model Sting Power Spectral Density Plot	38
16	Mach Number Profile for Five Hole Probe (Run 17Y-R6D)	39
17	Mach Number Profile for Flow Survey Model (Run 9A-A1)	40
18	Wing Pressure Coefficients for Mach 0.6 and 0.7	41
19	Wing Pressure Coefficients for Mach 0.8 and 0.85	42
20	Wing Pressure Coefficients for Mach 0.9 and 0.917	43
21	Center Body Pressure Coefficients for Mach 0.6 and 0.7	44
22	Center Body Pressure Coefficients for Mach 0.8 and 0.85	45
23	Center Body Pressure Coefficients for Mach 0.9 and 0.917	46
24	Shadowgraph of Flow Survey Model at Mach = 0.917	47

LIST OF TABLES

Table		Page
1	Model Airfoil and Orifice Locations	21
2	Pitch Plane Flow Angularity Values	22
3	Summary of IDS 7317 Accelerometer Measurements	23

I INTRODUCTION

The Holloman High Speed Test Track located in the Tularosa Basin of New Mexico has accommodated many types of aerodynamic tests since it began operation in the middle of the 1950's. These tests have ranged in velocity from low subsonic speeds to the near hypersonic regime and the sleds involved have carried payloads from as light as a few ounces up to thousands of pounds. The range of payload sizes has extended from as small as an air to air missile fin to as large as the entire forward section of a B-52 aircraft. The test objectives have included collecting steady state and transient aerodynamic and aeroelastic data on aircraft and missile panels, stabilizing components, control surfaces, etc. Other types of rocket sled applications which have provided aerodynamic information include tests of aircraft crew escape seat and pod ejection systems of parachute and associated drogue devices of rocket nozzle and plume effects, the measurement of skin temperatures, and the study of shock on shock interaction and other blast intercept phenomena (ref. 1). While many of these aerodynamic tests were conducted in the transonic range, they generally were not performed on a track vehicle specifically designed for transonic testing. For the past several years, however, the high speed Test Track has been developing data gathering techniques and rocket sled vehicles specially designed for application in the transonic regime. One such technique particularly suited for testing of semi-span or half models has recently been completed. These tests provided transonic information on a two dimensional panel model representing the essential features of an airfoil of a large transport aircraft (ref. 2). Recently the Test Track has also been

testing a rocket sled vehicle specially designed to carry large three dimensional models in the transonic range. This vehicle supports the model far ahead of the main sled structure approximately seven feet above the rail top surface, and moves it through the air at the track's elevation of 4,000 feet above sea level, at velocities in excess of Mach 1.2. It is anticipated that this vehicle will eliminate or at least minimize some of the difficulties encountered in transonic wind tunnels such as boundary layer buildup, flow angularity and blockage. As wind tunnel model size and angle of attack increase, these problems become increasingly severe and the resultant tunnel data cannot always be adequately adjusted. The following report presents both aerodynamic and vibration data obtained on this rocket sled while traversing the Holloman High Speed Test Track at transonic velocities.

II EQUIPMENT AND PROCEDURES

A. ROCKET SLED: The dual rail rocket sled, designated FDN 7314, was used to carry the payloads discussed in this report and is shown in Figure 1. It was specifically designed for transonic track testing of large three dimensional models. The sled was designed around a compromise between sled structural stiffness, sled frontal area and aerodynamic cleanliness, to minimize translational and rotational deflection of the sled/model interface and to produce minimal aerodynamic disturbances forward of this interface at all Mach numbers. The location of the sled/ model interface and the distance from this interface to the nearest point on the sled and track facility is shown in Figure 2.

As is standard practice at the test track this vehicle has a gap between the railhead and the slipper which is attached to the sled and

grips the railhead. This gap can be a maximum of 0.125 inch when the slipper is touching any one surface and measured at the opposite surface. As a result of this and the 216 inches between slipper beam centerlines the vehicle can be at yaw or pitch attitudes up to $\pm$.033° depending on the overall sled loading conditions being experienced. Winds encountered along the sled trajectory may also necessitate attitude corrections. This effect on sled yaw angle is graphically shown in Figure 3. In order to minimize these effects, sled tests of this nature are not run above 5 knot winds.

The vehicle has a gross weight of 6,475 pounds which includes the 75 pound model payload and 150 pounds of transducers, power supplies, electronic signal conditioning and telemetry equipment, pallets, containers and the associated vibration isolation system. The telemetry equipment and other necessary electronic hardware are carried in three compartments located in the twenty-four inch diameter cylinder which forms the upper part of the rocket sled.

The vehicle is capable of being pushed to Mach 1.5 by lower stage propulsion units which are left behind allowing FDN 7314 to sustain its velocity and/or coast to a stop by itself. The free-run may be terminated at the lower velocities if necessary by the momentum exchange water brakes located forward of the front slippers on each rail. The sled is able to sustain its velocity at several discreet levels through the simultaneous firing of two or more of the nine on board rocket motors. The discreet sustain velocities are determined by matching the nine incremented thrust levels with combined drag of the vehicle and model payload. Velocities may be sustained for up to five seconds.

The instantaneous sled velocity relative to the track is calculated from time and distance data measured by an electro-optical system which is standard at the test track for dual rail rocket sled vehicles (ref. 3). Mach numbers calculated from data obtained by this system can be corrected for wind induced errors if these errors are above the noise level. This electro-optical system is located on the starboard rear slipper beam end.

As was previously mentioned, the sled was designed to minimize aerodynamic disturbances in the vicinity of the model and thus has a projected area when viewed from the front of 10.4 square feet, which is relatively low for rocket sleds of this weight. The sled has a subsonic drag coefficient (C_D) referenced to this frontal area of 0.67 and a drag coefficient of 1.0 at Mach 1.

B. FIVE HOLE DIRECTION PROBE: The five hole direction probe used during this run series and the related support assembly are shown in Figure 4. The probe was obtained from AEDC. It has been calibrated in the AEDC Aerodynamic Wind Tunnel (1T) at pitch and yaw angles from -4 to +4 degrees and Mach numbers from 0.5 to 1.5. A detailed description of the calibration method can be found in reference 4. The probe has forty inches of stainless steel tubing leads with 0.036 inch inside diameters. Five, 17-foot strands of flexible plastic tubing with .043 inch inside diameter connects the steel tubing leads to five Bell & Howell, type 4-312-002, pressure transducers which were installed on a vibration isolated pallet in the forward instrumentation compartment of the rocket sled. The longitudinal axis of the pressure transducer is oriented in the cross track direction to eliminate sled boost acceleration sensitivity. The transducers connected to orifices 1 through 4 (Figure 4) had a range from 0 to 7.5 psi and the transducer connected to orifice 5 had a range of 0 to 12.5 psi. The reference sides of the five pressure

transducers were connected to a common pressure reservoir which was vented to the atmosphere and closed just prior to each run. The transducer output signals were digitized through a pulse code modulation unit and transmitted to the ground station by FM telemetry. The direction probe assembly was aligned parallel to the ground while the rocket sled was sitting on a special fitting track located in the track fabrication shop. The vehicle slipper gap was equally shimmed to align the sled with the fitting track. An optical tooling jig transit was used to obtain the attitude of the probe relative to a plane passing through the rail's top surfaces. These measurements indicated that the probe was installed with 0.087° yaw to the port and 0.062° pitch up attitude.

C. ACCELEROMETER INSTALLATION: The accelerometer measurements discussed later in the report were taken with 2262-200 Endevco piezo resistive accelerometers. These instruments are capable of a 1,000 Hz frequency response which was accommodated by a constant bandwidth FM/FM telemetry system. The accelerometers were placed in three mutually orthogonal directionals and mounted on the base of the cone shown in Figure 4.

D. FLOW SURVEY MODEL: The flow survey model installed on the sled is shown in Figure 5. Basic model dimension, calibration loading points and strain gage and orifice locations are shown in Figure 6 and Table 1. The model contained 44 wing orifices located 8 inches out from the center body centerline. Twenty-two orifices were located on the underside of the port wing and 22 orifices were located on the top side of the starboard wing. The orifices were located at the following percentages of wing chord: 0, 2.5, 5.0, 7.5, 10.0 and each 5 percent increment up to 95%. The wing

orifices had a diameter of .0225 inch and were located at the points shown in Table 1. The center body contained twelve orifices on the top centerline and twelve orifices on the bottom centerline. Each of these orifices was .024 inches in diameter. Both wing and center body orifices were connected to stainless steel tubing with an inside diameter of .024 inches. Each stainless steel tube was ten feet in length and was in turn connected to eleven foot lengths of flexible plastic tubing with an inside diameter of .043 inches.

The plastic tubing was connected to the pressure transducers which were installed on two vibration isolated pallets in the forward instrumentation compartment of the rocket sled. The transducers had four different pressure range capacities (i.e., 3.0, 5.0, 7.5 and 12.5 psi). The maximum anticipated pressure level of each orifice determined which of the four ranges were used. The reference sides of the set of transducers which had the same pressure range were connected to a common pressure reservoir which was vented to the atmosphere just prior to each run. The transducer output was sent through a pulse code modulation unit to digitize the signal and the resultant signal transmitted to the ground station by FM telemetry.

An 0.1 inch wide boundary layer trip was applied to the full span of the model wing at the 5% chord line. The trip was developed by bonding a sprayed layer of 0.007 inch diameter glass shot to the wing surface. The model was aligned in the same manner as the five hole direction probes and was positioned to less than 0.01° in pitch and yaw, relative to two mutually perpendicular planes one of which passes through the rail top surfaces and the other one vertical, pointing in a down track direction. The sting support was strain gaged in the two locations shown in Figure 6

with two independent 120 ohm Wheatstone bridges. Each bridge was calibrated as a function of angle of attack. The results of this calibration are shown in Figure 7. Four lines are presented in this figure. The two upper lines refer to the gage closest to the model and show the small dependence of the millivolt output on point of load application (i.e., 8.484 and 12.484) for a common angle of attack ($\alpha°$). The two lower lines present similar information on the gage nearest the sled. As is indicated in the figure the full scale value used in the sled run data was higher than the actual calibration. The increase was necessary to prevent over deviation of the data by track/sled dynamics.

III RESULTS AND DISCUSSION

A. FLOW ANGULARITY

1. Five-Hole Direction Probe: Two rocket sled runs were conducted with a five-hole direction probe provided by AEDC. The probe and interface structure is shown in Figure 4. The data were obtained through the use of the telemetry system previously described. The first run did not provide useful flow angularity data due to loosening of the probe at some time during the run. The second run did not encounter any structural or data acquisition problems and provided useful pressure information. The following is a tabulation of the pressures measured at selected Mach numbers during the sled run:

M	P_1	P_3	P_2	P_4	P_5
0.7	1.6011	1.7168	1.7812	1.7866	5.1381
0.8	2.5383	2.6532	2.7492	2.6410	6.8179
0.85	3.1631	3.2775	3.4075	3.2625	7.8060
0.9	3.7880	3.9018	4.0271	3.9616	8.8929

This pressure information was applied to three different methods for calculating flow angularity.

The first method applied a system of calibration equation to the pressure data obtained during the sled run. A simplified form of the equation for the vertical plane is

$$\alpha = J\left[\frac{P_2 - P_4}{P_5}\right] - K\left[\frac{P_3 - P_1}{P_5}\right] + \varepsilon_o$$

where the constants for specific Mach numbers (M) are

M	J	K	ε_o
0.7	3.3114	-53.800	-0.4182
0.8	3.9862	-49.370	-0.3755
0.85	3.7108	-47.080	-0.4083
0.90	2.9079	-45.610	-0.4200

The value ε equal to approximately -0.4 degrees indicates that an observer fixed to and moving with the model would view the approaching flow coming from above and moving toward the ground. This flow angle is not considered plausible under existing sled run conditions. This term is interpreted as a correction for a built-in fabrication error of this specific probe. This equation and the above calibration constants were provided by AEDC. The flow angularity in the pitch plane as determined using the previously described information is listed in column 3 of Table 2. The significance of the angle will be discussed following the detailed description of the two other methods used to determine the other values presented in the table.

Figure 8 presents the flow angularity versus Mach number. This graph is included in this report primarily for the purpose of demonstrating the

results of the digitizing process used. The data points indicated in this figure were obtained using a more general form of the previous equation, a larger sampling of the pressure data and a computer routine. The stratification of the points into three levels is the result of the digitizing process and instrumentation accuracy. The digitizing process requires that the calibration level for P_1 through P_4 which in this case was 5.0 psig be divided into 256 discreet steps. Thus each of the resulting steps is approximately .0391 psi, and these steps when applied to the equations result in the distinct stratification noted in the data.

The second method for determining flow angularity in the pitch plane using the measured pressure was obtained from reference 5. The flow angle is given by the following equation:

$$\alpha = \frac{P_3 - P_1}{P_5 - P_3} \left[\frac{2}{9\sin 2\theta} \right]$$

For the probe used in this report θ is equal to 40°. This is the angular location of the orifices in the pitch plane. The results of these calculations are presented in column 1 of Table 2. It should be pointed out that no effort was made to correct the flow angle calculated by the above equation for fabrication errors.

A third method of calculating pitch plane flow angularity was obtained from reference 6 which provides the following equation:

$$\alpha = \frac{P_3 - P_1}{P_5} \times \frac{1}{a}$$

In this equation "a" is the linear sensitivity per degree and is given in the following table:

M	a[deg^{-1}]
.7	0.0728
.8	0.0645
.85	0.0603
.9	0.0560

The results of calculations using the above information are listed in column 2 of Table 2. Again no attempt was made to correct for fabrication errors.

In comparing the angle of flow calculated by the above methods it is evident that the results of the first method (column 3, Table 2) do not agree well with the other two methods at the lower two Mach numbers. particularly since no effort was made to account for the fabrication errors in the results of the last two methods (columns 1 and 2 of Table 2). The values presented in columns 1 and 2 of Table 3 are identical except for a scale factor. The values listed in column 3 show a completely different trend than those in the other two columns. The values presented in columns 1, 2 and 3 have not been corrected for the 0.062° pitch up misalignment discussed in paragraph B of this report. The positive flow angle listed in Table 2 indicates that relative to an observer fixed to the probe tip the flow is coming from below and moving upwards.

2. Flow Survey Model: One rocket sled run was conducted with a flow survey model provided by AEDC. The model installation is shown in Figure 5. Two methods were applied to the measured data in calculating flow angularity. The first method used the most forward upper and lower pressure obtained on the center body to calculate the flow angularity experienced during the run. First the pressure coefficient (C_p) for the upper and lower orifice was

calculated by dividing the gage pressure measured at each orifice by the dynamic pressure (q). The dynamic pressure was obtained using the ambient static pressure and temperature measured at the Track facility that day and the velocity obtained from the electro-optical time and distance data measured during the run. The resulting pressure coefficients are presented in Figure 9 for a selected time interval. It should be pointed out that the indicated pressure coefficient drop on the upper center body at approximately 8.92 seconds is caused by the digitizing process. For example, the pressure transducer for that orifice is calibrated for ±5.0 psig and therefore, each of the 256 digitized steps is equal to .039 psig. For a change in pressure of this amount the pressure coefficient C_p would change by approximately .006. Since the pressure transducer is accurate to approximately 0.04 psi, the digitizer output could jump by two steps or a change in C_p of approximately 0.012. The pressure coefficients beyond 11.52 seconds exhibit an apparent upward slope over short time increments. This results from the fact that the indicated pressure reading remains constant at one digitized step for a time interval Δt during which the transducer output changes sufficiently to cause the digitizer to jump to the next step. During this time interval, however, the dynamic pressure readings change continually, so the indicated digitized pressure is divided by decreasing values of q, causing the apparent rise in C_p. A difference between the upper and lower C_p of .006 was estimated from the data presented in Figure 9. The differential pressure coefficient was the inserted to the following equation.

$$\alpha = A_o + A_1 \left[C_{p_L} - C_{p_u} \right]$$

where the constants for selected Mach numbers (M) are:

M	A_o	A_1
0.7	0.182	17.984
0.8	0.130	16.868
0.85	0.144	17.158
0.9	0.124	18.095

The equation and list of constants were provided by AEDC. The flow angularity calculated using the above information is presented in column 4, Table 2. Flow angularity was also calculated from pressures measured on the model wing. Wind tunnel data were available for the wing pressures at various angles of attack. From these data a C_p was obtained for a change in angle from 0° to 2° and it was assumed that the C_p would vary linearly through this range for the first two orifices near the wing leading edge. Dividing the pressure differential obtained from the pressures measured at the second orifice back from the leading edge of the upper and lower wing surface by the assumed value of change in pressure coefficient per degree for each Mach number, the angles in column 5 of Table 2 were calculated.

3. Survey Model Sting: During the sled run on which the flow survey model pressure measurements were obtained, strain gage measurements were made on the sting supporting the model. These measurements were taken on two independent strain gage bridges. The data were put on two constant bandwidth channels having 4 KHz response. The measurements therefore, contained dynamic information on the test assembly and are discussed in another section of the report. For purpose of determining the quasi steady state flow angularity the information was filtered at two cycles per second. The resulting angular deflections determined by this technique are presented in Figure 10. From this figure the average angle was selected for each Mach

number of interest and is listed in column 6 of Table 2. Obviously this angle represents an angular alignment change due to sting deflection, not an angular deviation of the approaching flow.

B. ACCELEROMETER DATA

The accelerometer data to be discussed are taken from measurements made on five sled runs. The three accelerometer locations are shown in Figure 4. The first three runs (i.e., 17Y-R1, 17Y-R3 and 17Y-4B) were conducted without the five hole direction probe, and the extension tube forward of the cone was not installed. The remaining two runs were performed with the probe and extension in place. The 9^{o} half angle cone was in place on all runs. Figures 11, 12, and 13 present the power spectral density (PSD) plots of the vertical, lateral and longitudinal accelerometer data obtained during Run 17Y-R6 between 6.88 to 7.88 seconds. The PSDs were obtained from data which were converted from analog to digital information at a sampling rate of 4,096 points per second. The data are not continuous as plotted but consist of a series of connected points. To obtain these points the accelerometer information was filtered with a 2 Hz bandwidth filter from 0 to 100 Hz, with a 4 Hz bandwidth filter from 100 to 200 Hz and with a 6 Hz bandwidth filter from 200 to 2,000. This process produces one point for every 2 Hz, 4 Hz and 6 Hz in the respective frequency ranges. A summary of the results of all runs is shown in Table 3. The G_{RMS} listed in the X-direction do not contain the bias due to the slow varying boost or coast acceleration value. In order to obtain information on some of the natural frequencies of the sled structure, the tabulated data plotted in Figures 11, 12, and 13 were examined. Each frequency at which a maximum occurred was considered a modal frequency, and for each frequency which exhibited the maximum power, the z and y direction were considered to be the downtrack, vertical plane (i.e. vertical) and the cross track, vertical

plane (i.e. lateral) respectively. These are listed below as the primary plane of the particular mode shape. The following list contains measured frequencies and frequencies obtained from a structural dynamic computer solution of a mathematical model developed for this specific rocket sled.

Mathematically Predicted Hz	Measured During Runs Hz
12.4 Lateral	14 Lateral
17.2 Vertical	19 Vertical
26.1 Lateral	24 Lateral
35.6 Vertical	31 Vertical
41.2 Lateral	40 Lateral
44.8 Vertical	45 ?
71.1 Lateral	60 ?

The last two frequencies cannot be determined in this manner since the power level is approximately equal in each direction. The mathematically predicted frequencies listed are the first seven mode shapes determined by the computer solution and have no imbedded frequencies omitted.

C. STING STRAIN GAGE DATA

The data discussed in this section were obtained from the strain gage bridges installed on the flow survey model sting in the location shown in Figure 6. Figure 14 presents a sample of the sting and model response to forcing functions produced by the track environment. In this figure, a slight bias can be observed. This is considered to be the quasi-steady state angular deflection. Figure 15 presents the power spectral density for the forward strain gage for a time segment of 8.155 to 9.155 seconds. This figure is representative

of the data obtained on the aft bridge. The analog information was digitized at 4,096 points per second for data presented in this figure. The PSD was obtained using a 6 Hz bandwidth filter through the entire frequency range. From the PSD it can be seen that one or two distinct resonant frequencies exist between 12 and 24 Hz. Close examination of the type of data shown in Figure 14 indicates a frequency at approximately 14 Hz. A mathematical approach using an equation of the form obtained from reference 7 for a cantilevered beam with concentrated and distributed masses

$$\omega_n = \left[\frac{3EI}{\ell^3 (m+.23m_b)}\right]^{1/2}$$

results in a calculated frequency of 29 Hz. To obtain this value, the moment of inertia (I) of the sting was estimated to be 0.9 in^4. Since the sting is composed of a straight and tapered section as shown in Figure 6 the exact value of (I) cannot be obtained readily by a simple analytical approach. The mass of the model (m) and sting (m_b) are 0.65 and 0.61 $lb\text{-}sec^2/in$, respectively. The length (ℓ) is 31.0 inches. From this calculation it is evident that the previously determined resonance at 14 Hz is not a sting mode but most likely the influence of one or both of the two sled frequencies 14 and 19 Hz as determined from the accelerometer measurements. However, because of the limited accuracy of both the analytical and measured frequency it cannot be determined whether the frequency indicated to be around 24 Hz in Figure 15 is a frequency of the sting, sled or sting-sled interaction. In future tests all efforts will be made to assure separation of sting and sled frequencies.

D. MACH NUMBER MEASUREMENTS

During the test at which the pressure data were obtained, measurements were made which allowed Mach number to be calculated by two completely different techniques. The standard technique at the Test Track for calculating Mach number on all dual rail rocket sled runs is to divide the velocity obtained by the electro-optical space time system by the speed of sound. The speed of sound in feet per second is calculated for the ambient air temperature of the facility at the time of the run through the use of the following equation:

$$a = 49\ (T+459.6)^{1/2}$$

where T = temperature in degrees Fahrenheit.

The results of the calculations using this standard technique are shown in Figures 16 and 17 for runs 17Y-R6 and 9A-A1, respectively. The solid line in both figures is obtained by fairing through all data points provided by the electro-optical system. The dots depicted in these two figures are obtained by a second technique which uses the following equation taken from reference 8.

$$M = 5\left[\left[\frac{PTP}{P_s}\right]^{.2857} - 1\right]^{1/2}$$

The pressure (P_s) is the ambient static pressure at the facility at the time of the run. PTP is the total pressure which is obtained by adding the ambient pressure to the stagnation pressure. The stagnation pressure is measured at the center orifice in the five hole direction probe and resulting calculations shown as dots in Figure 16. Figure 17 contains the result of using the stagnation pressure measured at the orifices located on the leading edge of the starboard wing of the flow survey model. The stepping of the data is caused by the digitizing process which was described previously. The Mach numbers

calculated by the second technique using the mean time for each of the digitized steps are within approximately 0.005 Mach of those calculated by the Track standard technique for the sustain phase and the coast phase at least down to approximately M = 0.6. The comparison of the Mach numbers obtained from the two techniques gives an indication of the pressure lag in the system. The Mach number determined by the electro-optical space time system is considered to be the true value at each time. During the boost phase the pressure lag in the system is evident, however the boost phase is generally not considered to be the prime data collection period.

E. FLOW SURVEY MODEL PRESSURE COEFFICIENTS

Pressure measurements were obtained at all Mach numbers during acceleration, peak velocity, sustain, and deceleration portions of the sled trajectory. The pressure coefficients calculated from the measurements taken on the wing of the flow survey model during sustain and deceleration are shown in Figures 18 through 20. Pressure measurements were taken on twenty orifices of the top surface of the starboard wing and twenty orifices on the lower surface of the port wing. The data points missing at the orifice on the upper wing at 20% chord and the lower wing at the 10% are due to problems associated with data reduction techniques. The missing data from the orifice at 75% chord for Mach 0.6 and 0.7 is a result of noise on the telemetry channel during this period of the run. Figures 21 through 23 present the pressure coefficients calculated from sled run data for the flow survey model center body. Pressure measurements were obtained from nine orifices on the centerline of the upper surface of the center body. The missing data at orifices located at 33.2%, 57.2% and 102.5% of the chord on the upper body surface and 102.5% on the lower wing are a result of plugged

orifice and/or tubing leading to the transducer. This condition was observed during checkout of the model prior to installation on the rocket sled by blowing smoke through the individual tubes. These orifices were left inoperative. Wind tunnel data provided by AEDC are superimposed on these figures but are not available for all Mach numbers. Comparing the wind tunnel data with the average pressure coefficient of the upper and lower wing which was calculated from the sled test data, makes it evident that the wind tunnel pressure coefficients in general are slightly higher and that for equal Mach numbers, the formation of a shock wave on the wing as indicated by an abrupt change in pressure coefficient occurs in the wind tunnel aft of the location where it occurs on the sled, as indicated by the pressure coefficients. Sled derived pressure coefficients are also presented for the peak Mach number of 0.917 reached during the sled run, and the shadowgraph obtained at this Mach number is shown in Figure 24. The upper part of this figure shows the flow model with the wing outline added to aid in locating the wing position. The lower portion of the figure shows the complete sting and its attachment at the interface of the sled.

CONCLUSIONS

1. The flow field forward of the sled/model interface has less than one quarter of one degree flow angularity from Mach 0.7 to Mach 0.9.

2. Mach number can be determined within 0.005 by either of two independent techniques. One technique uses the standard Test Track electro-optical space time measurement system and the other uses static and dynamic pressure measurements.

3. Pressure lag effects can be minimized by sustaining the rocket sled velocity during prime data collection periods.

4. Wind tunnel and track measured pressure coefficients compare closely with coefficients obtained on the track generally being slightly higher.

5. Shock waves as indicated by high pressure gradients in the data form farther from the wing trailing edge on sled tests than in wind tunnel tests.

REFERENCES

1. Rasmussen, Hans, J., High Reynolds Number Testing by Means of Rocket Sleds, AGARD Conference Proceedings Nr. 83 on Facilities and Techniques for Aerodynamic Testing at Transonic Speeds and High Reynolds Numbers, Paper Nr. 33, Gottingen, Germany, April 1971.

2. Rasmussen, Hans, J., Transonic Pressure Distribution on an Aircraft Wing Model During Rocket Sled Runs, ADTC-TR-77-34, 30 March 1977.

3. The Holloman Track, Facilities and Capabilities, ADTC, 6585 Test Group, Holloman AFB, New Mexico, 1974.

4. Baner, R. C., A Method for Calibrating a Cone-Probe Flow Field Measuring Instrument, AEDC-TR-69-201, November 1969.

5. Dean, Robert C., Jr., Flow Direction Measurements, Chapter V of Aerodynamic Measurements, M.I.T. Press, 1953.

6. Royal, B., Differential Pressure Measurements in Sensing Sideslip and Angle of Attack Proceedings of the Third International Symposium, Flight Test Instrumentation, Vol 3, Perganon Press, New York, 1964.

7. Harris, Cyril M., and Charles E. Crede, Shock and Vibrations Handbook, Vol I, McGraw Hll Book Company, Inc., New York, NY, 1961.

8. Equations, Tables and Charts for Compressible Flow, NACA Report 1135, U.S. Government Printing Office, Washington 25, D.C., 1953.

TABLE 1

MODEL AIRFOIL SHAPE AND ORIFICE LOCATIONS

Wing Airfoil Shape				Fuselage Orifice Locations
Chord	Thickness	Chord	Thickness	X/Chord*
.0000	.0000	3.6000	.2686	-0.738
.0450	.0445	4.0500	.2623	-0.680
.0675	.0535	4.5000	.2509	-0.564
.1125	.0679	4.9500	.2352	-0.448
.2250	.0940	5.4000	.2156	-0.332
.4500	.1302	5.8500	.1929	-0.216
.6750	.1572	6.3000	.1673	-0.100
.9000	.1790	6.7500	.1400	+0.131
1.3500	.2126	7.2000	.1123	+0.315
1.8000	.2368	7.6500	.0845	+0.572
2.2500	.2538	8.1000	.0567	+0.826
2.7000	.2648	8.5000	.0290	+1.025
3.1500	.2696	9.0000	.0117	

*Nondimensionalized by dividing by wing chord, with 0 being at the wing leading edge and (-) forward, (+) aft.

TABLE 2

PITCH PLANE FLOW ANGULARITY VALUES

Mach Number	1 Flow Survey Probe Ref 5 - EQ	2 Flow Survey Probe Ref 6 - EQ	3 Flow Survey Probe AEDC EQ	4 Model Body	5 Model Wing	6 Strain Gages on Sting
0.7	0.30°	0.40°	0.76°	0.29°	0.09°	0.06°
0.8	0.27°	0.35°	0.47°	0.24°	0.08°	0.09°
0.85	0.25°	0.32°	0.29°	0.24°	0.11°	0.14°
0.9	0.23°	0.29°	0.16°	0.23°	0.16°	0.20°

TABLE 3

SUMMARY OF

IDS 7317 ACCELEROMETER MEASUREMENTS

Run	t (sec)	Vel (ft/sec)	X G_{RMS}	Y G_{RMS}	Z G_{RMS}
17Y-R1	1.2 to 2.2	310→542	2.40	6.62	9.65
	2.7 to 3.7	559→545	2.98	8.46	15.83
17Y-R3	3.8 to 4.8	624→732	3.38	9.37	15.05
	5.2 to 6.2	726→704	3.66	10.45	14.69
17Y-R4B	2.4 to 3.4	710→927	4.49	9.67	14.59
	4.4 to 5.4	896→857	5.09	16.53	24.01
17Y-R5C	4.12 to 5.12	889→876	5.63	13.43	20.90
17Y-R6	6.88 to 7.88	1041→1020	4.72	11.88	14.67
	12.9 to 13.9	900→850	4.53	10.95	18.38

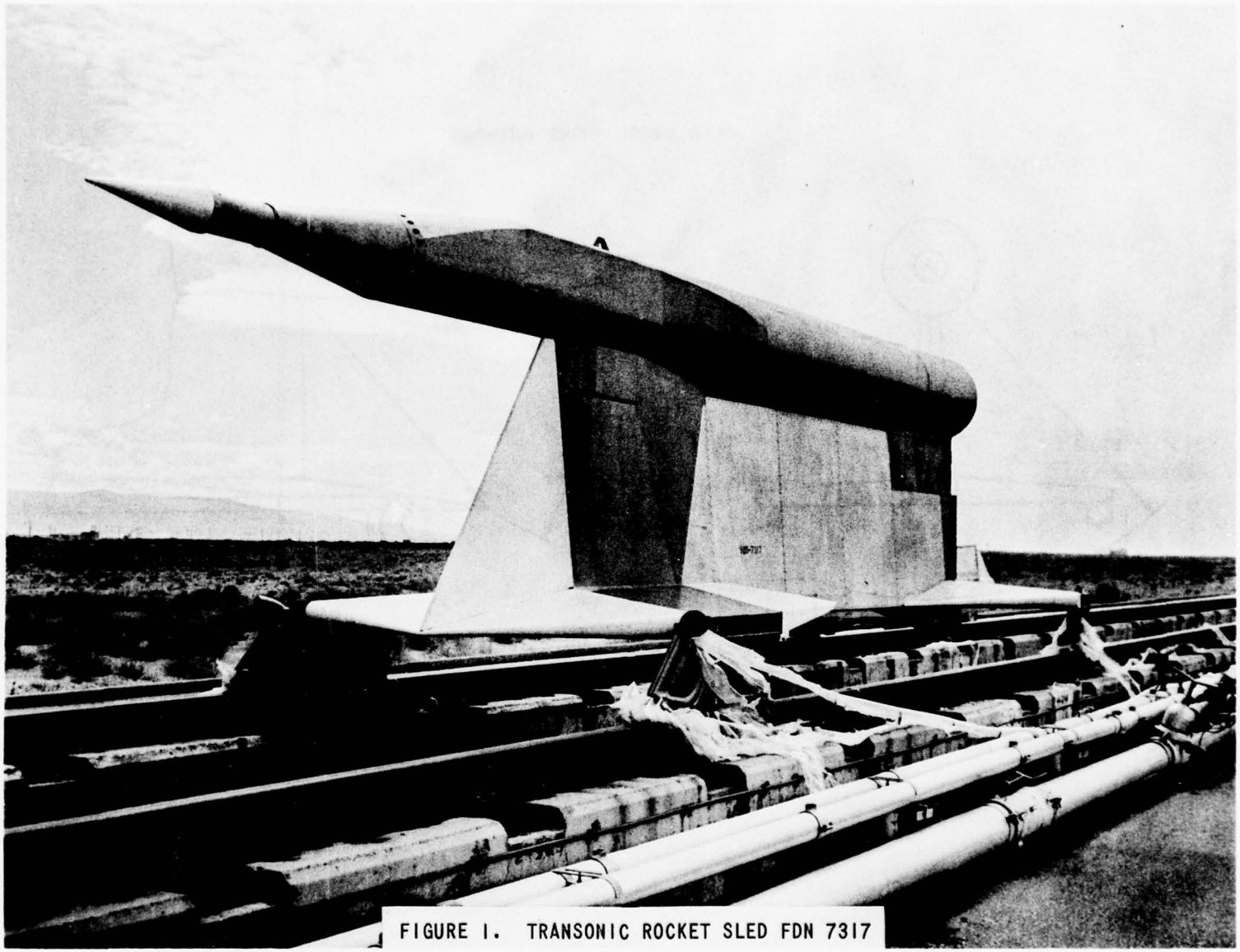

FIGURE 1. TRANSONIC ROCKET SLED FDN 7317

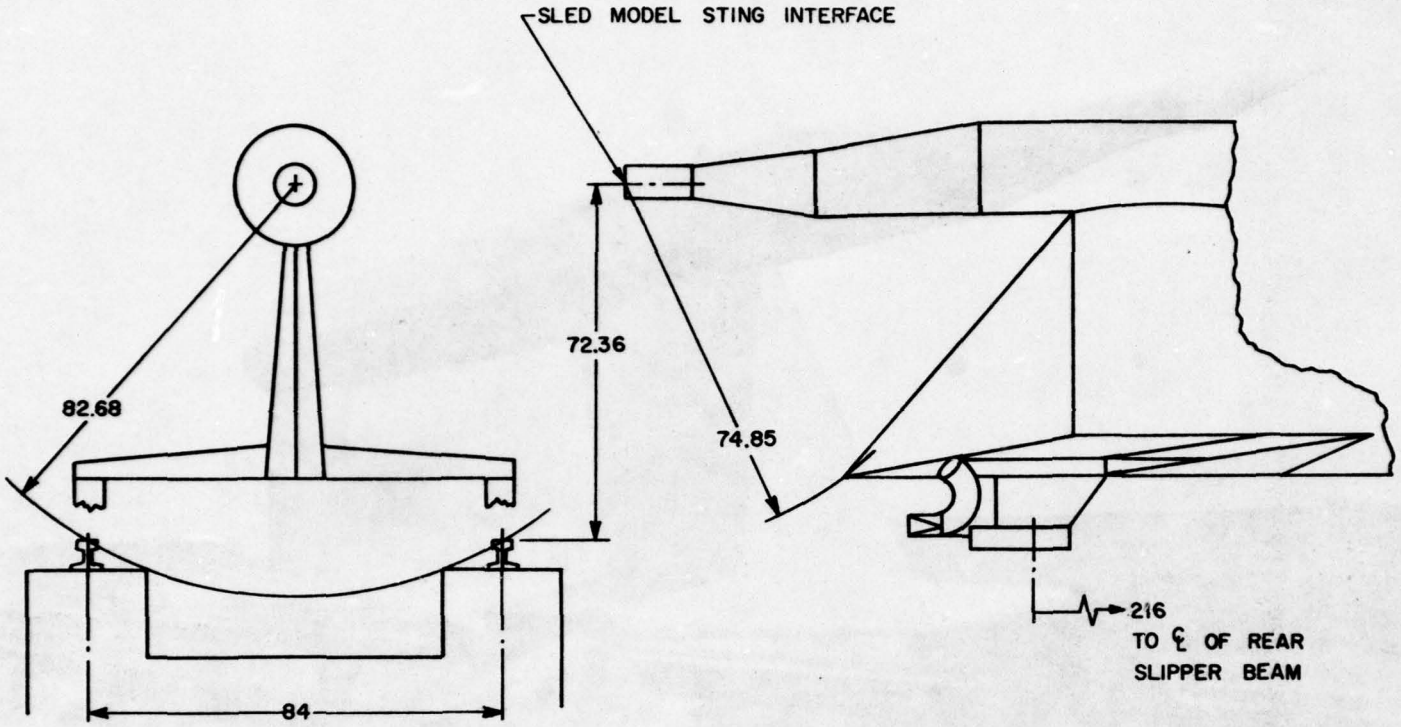

DIMENSIONS ARE IN INCHES.

FIGURE 2. SLED/MODEL INTERFACE LOCATION

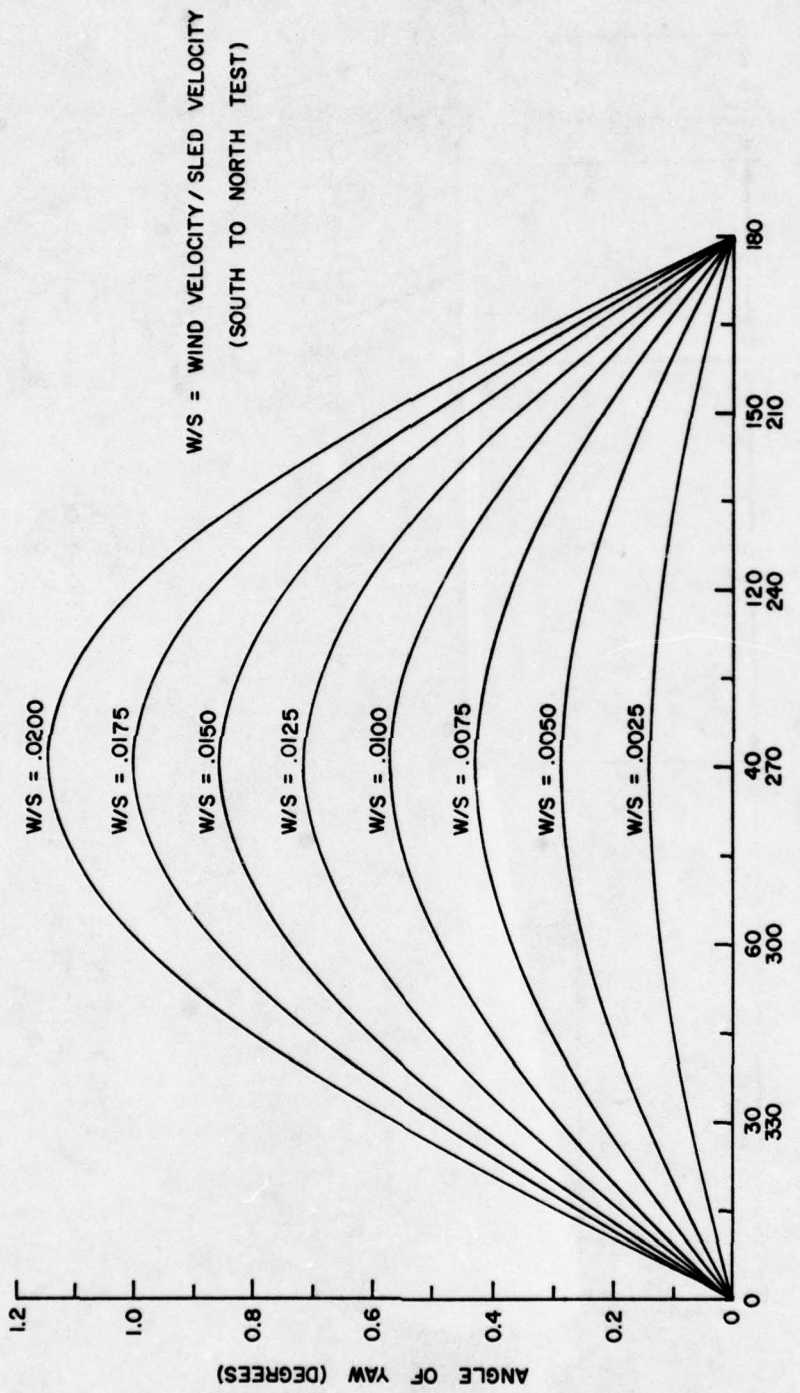

FIGURE 3. ANGLE OF YAW DUE TO WINDS VERSUS WIND DIRECTION

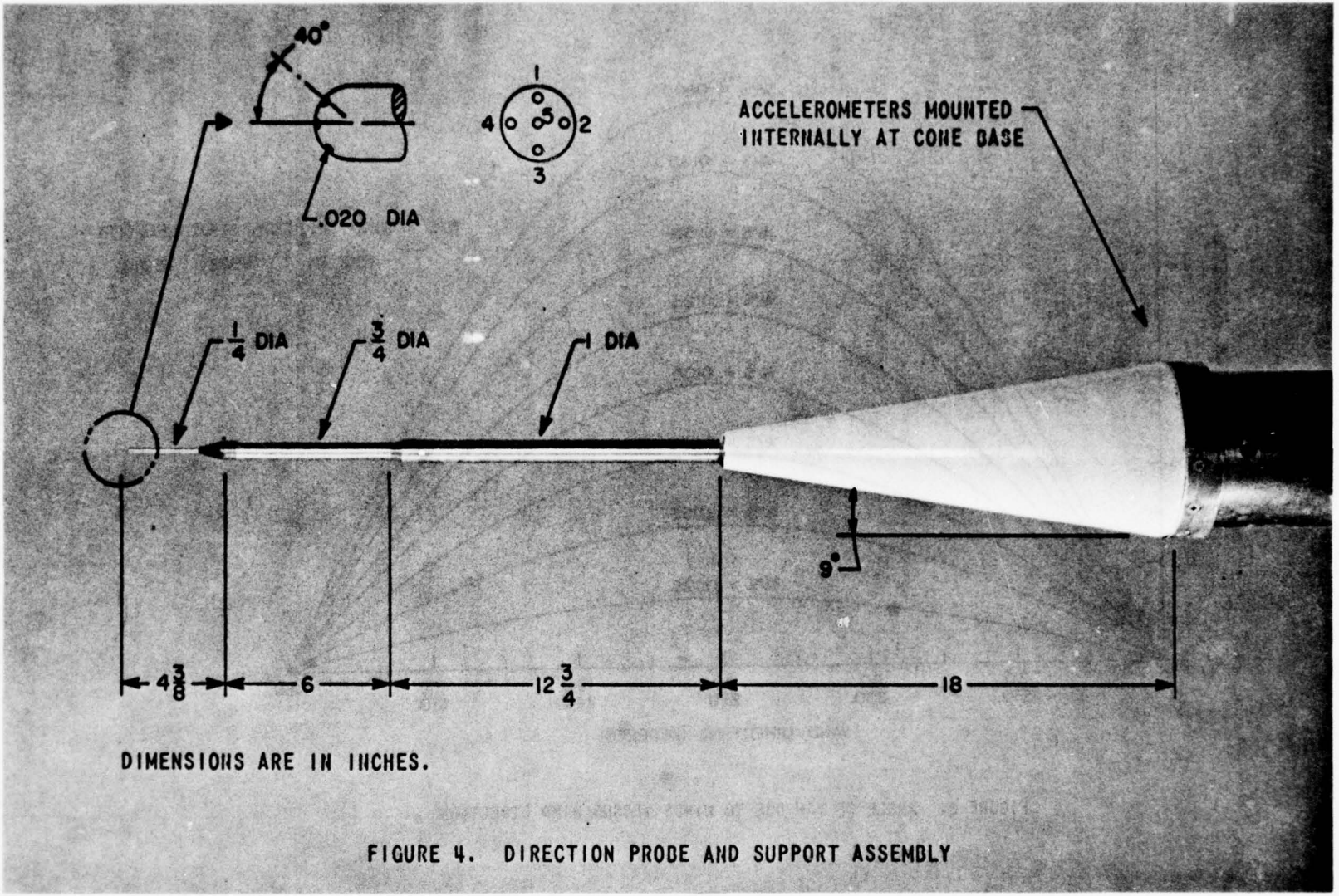

FIGURE 4. DIRECTION PROBE AND SUPPORT ASSEMBLY

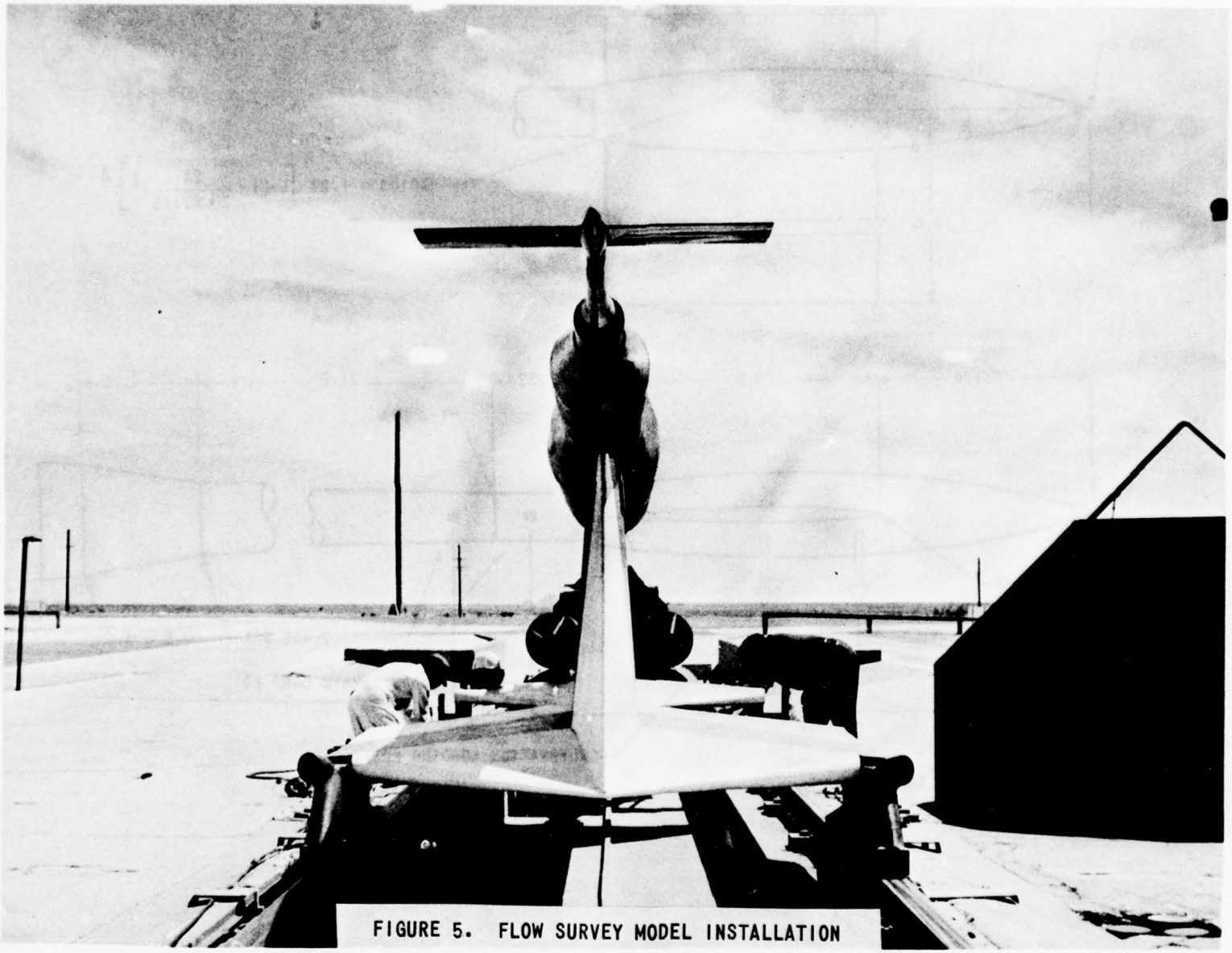

FIGURE 5. FLOW SURVEY MODEL INSTALLATION

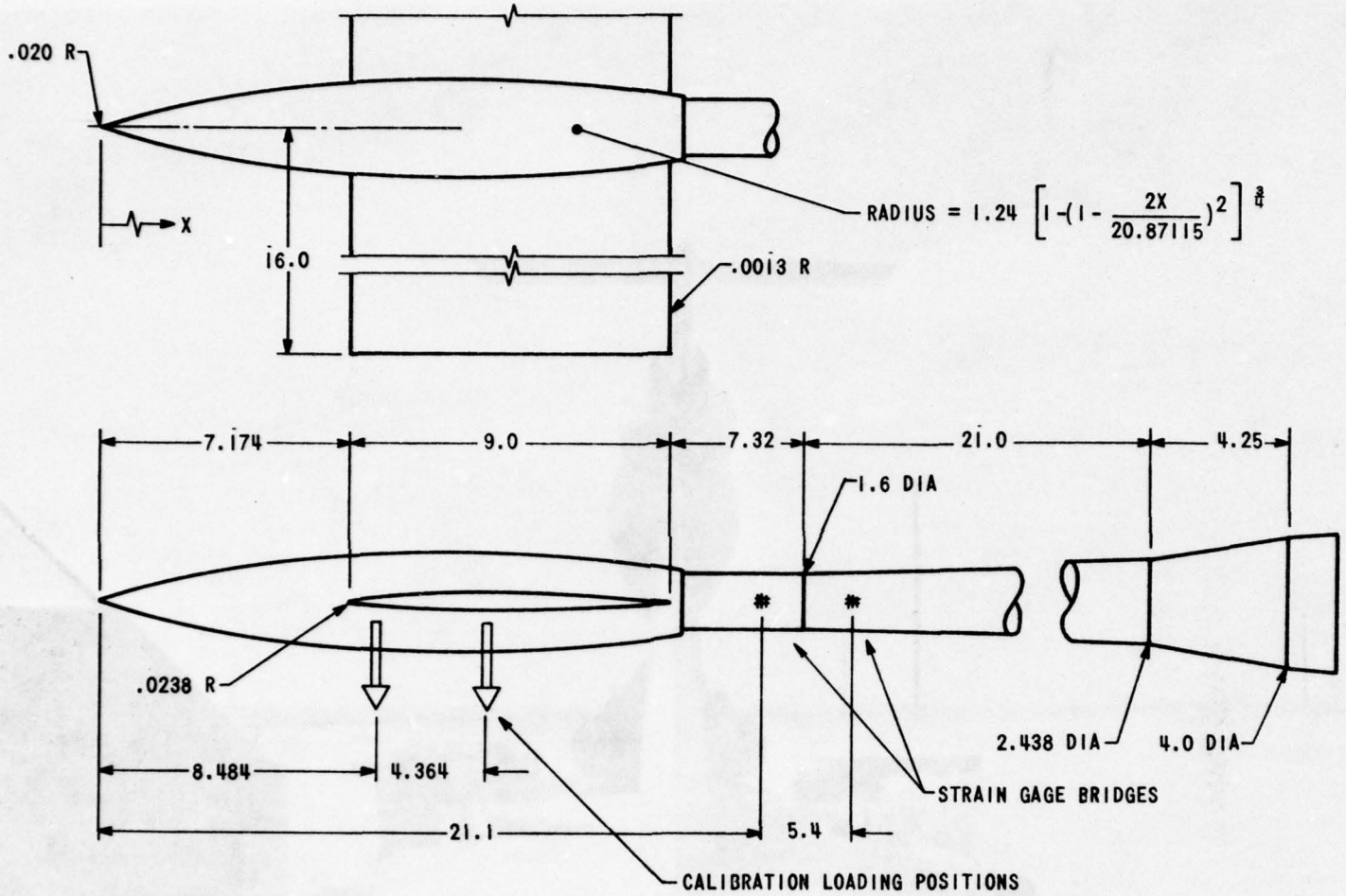

DIMENSIONS ARE IN INCHES.

FIGURE 6. FLOW SURVEY MODEL DIMENSIONS

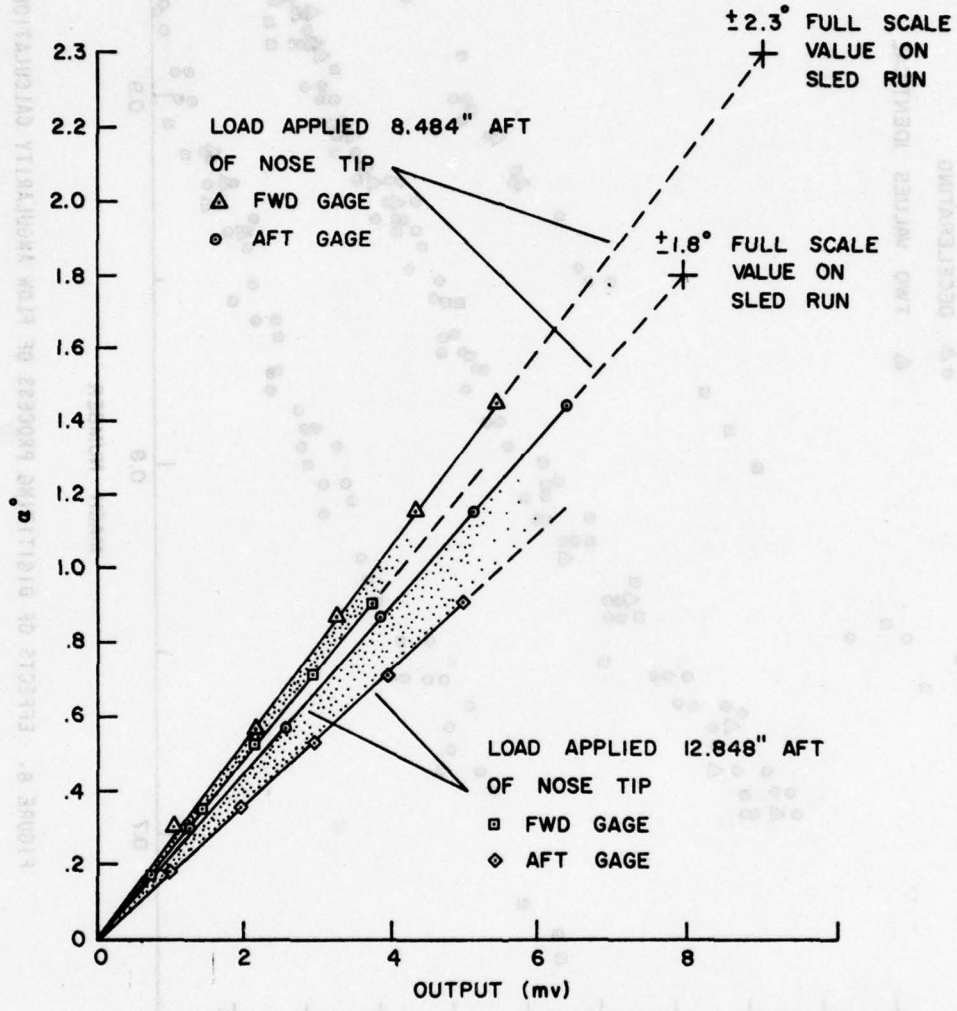

FIGURE 7. STING STRAIN GAGE CALIBRATION VALUES

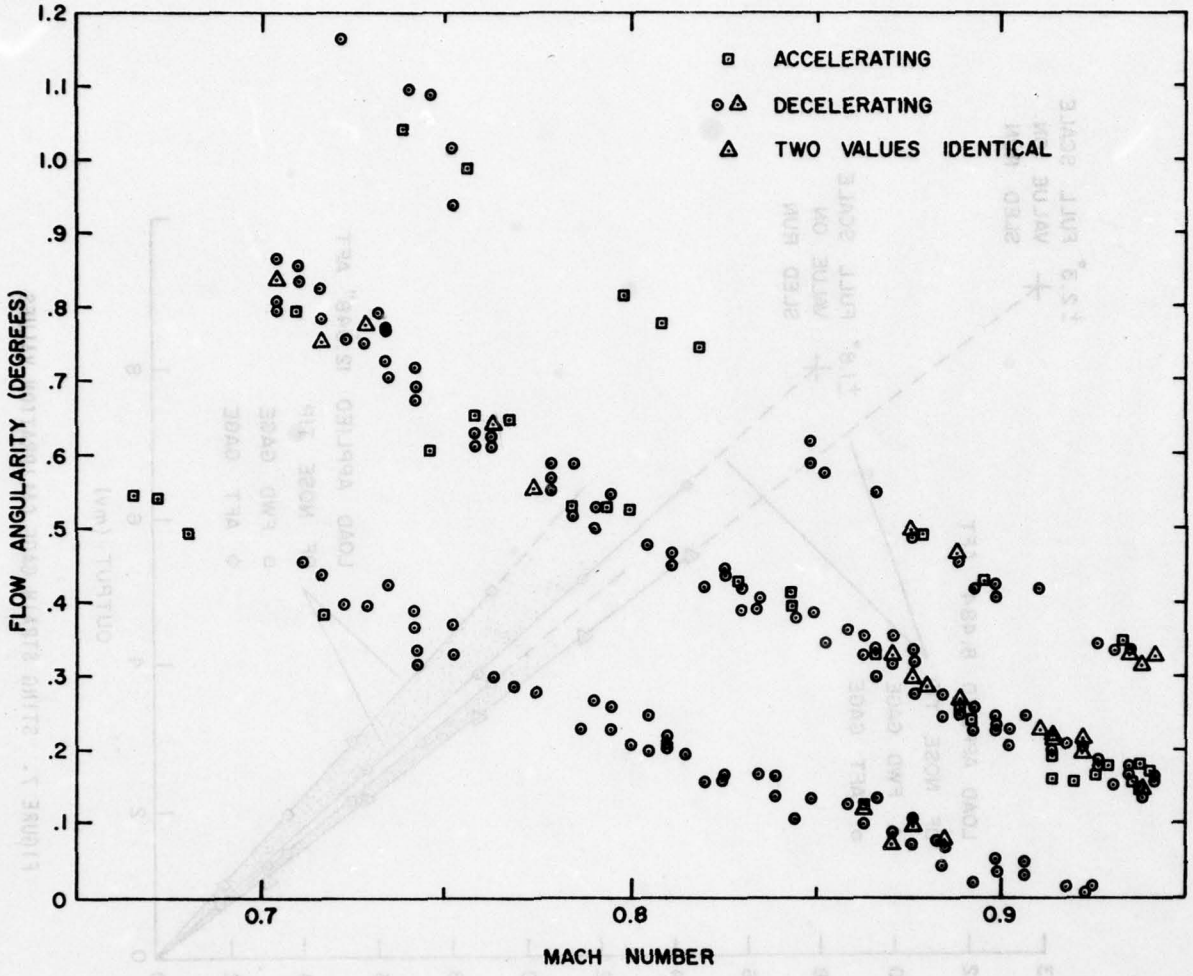

FIGURE 8. EFFECTS OF DIGITIZING PROCESS OF FLOW ANGULARITY CALCULATIONS

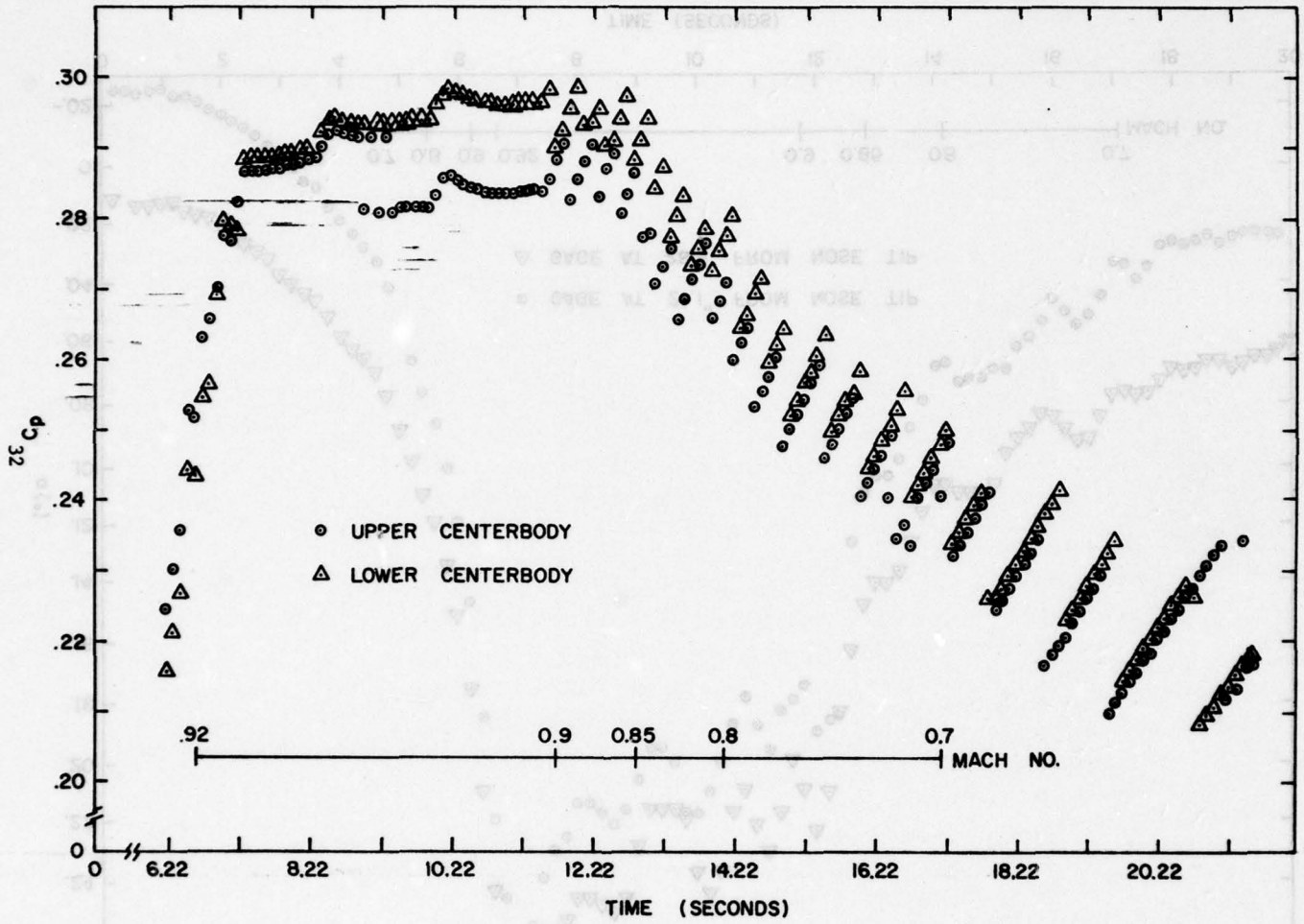

FIGURE 9. CENTERBODY PRESSURE COEFFICIENTS

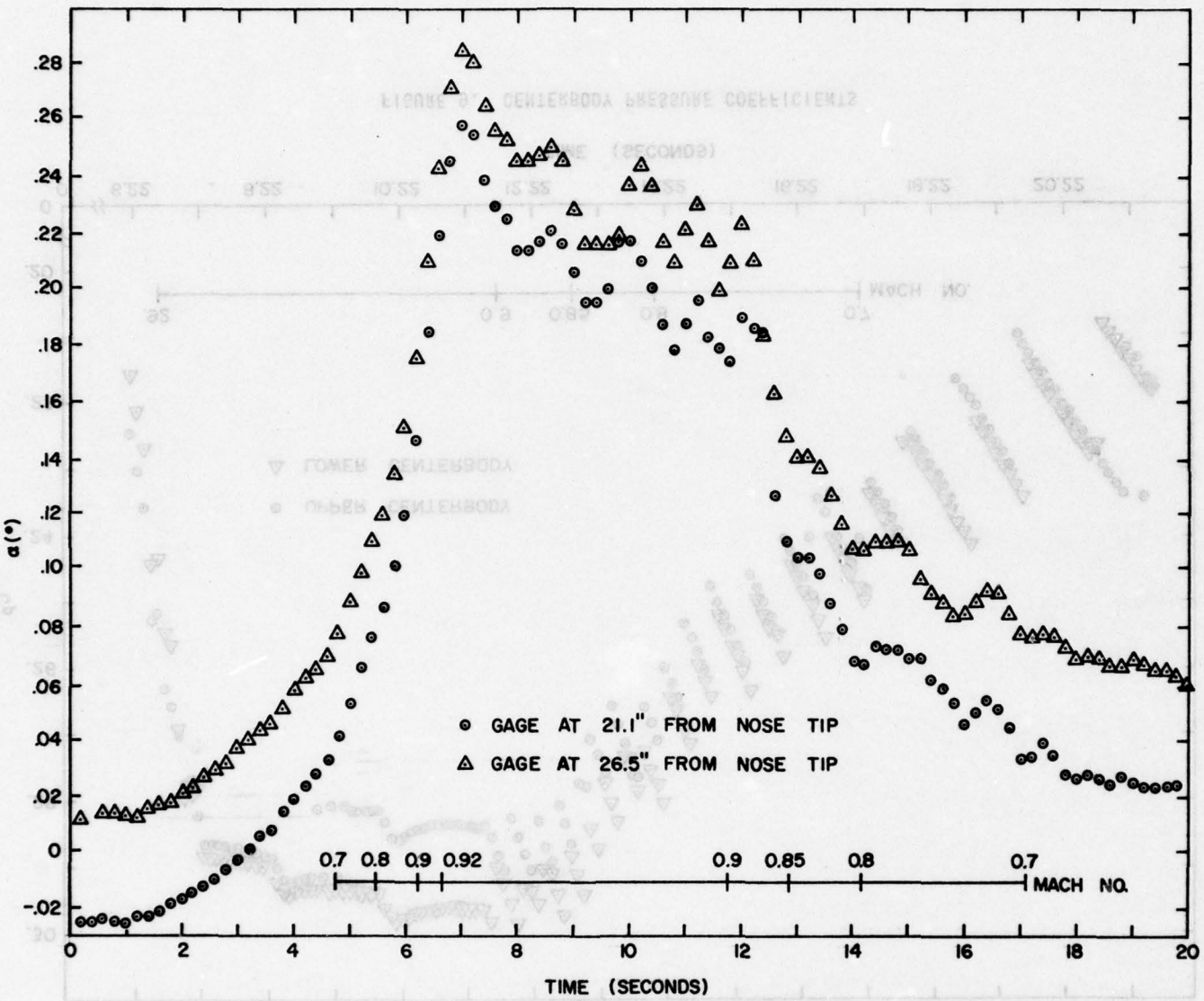

FIGURE 10. FLOW ANGULARITY DETERMINED FROM STING STRAIN GAGE DATA

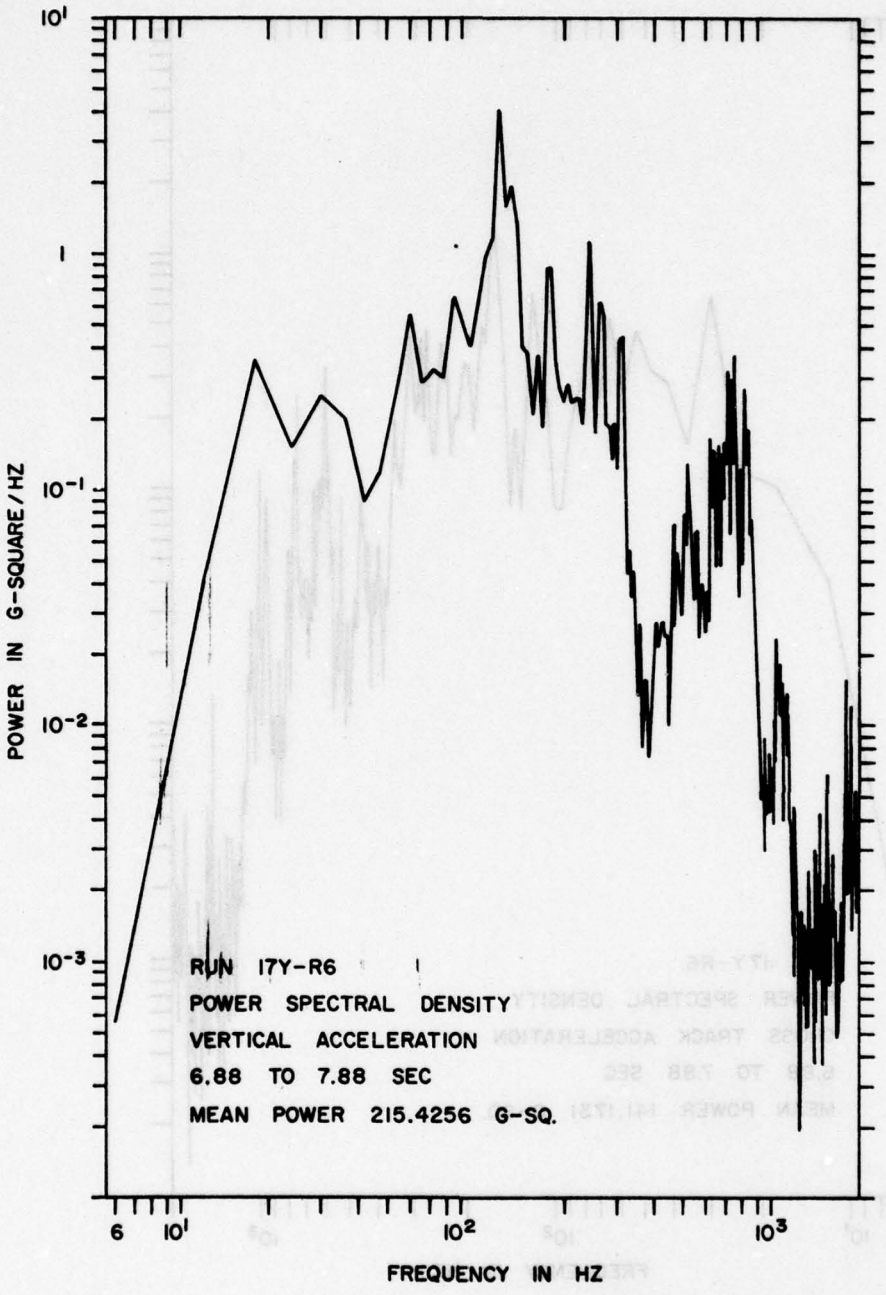

FIGURE 11. SLED/MODEL INTERFACE VERTICAL POWER SPECTRAL DENSITY PLOT

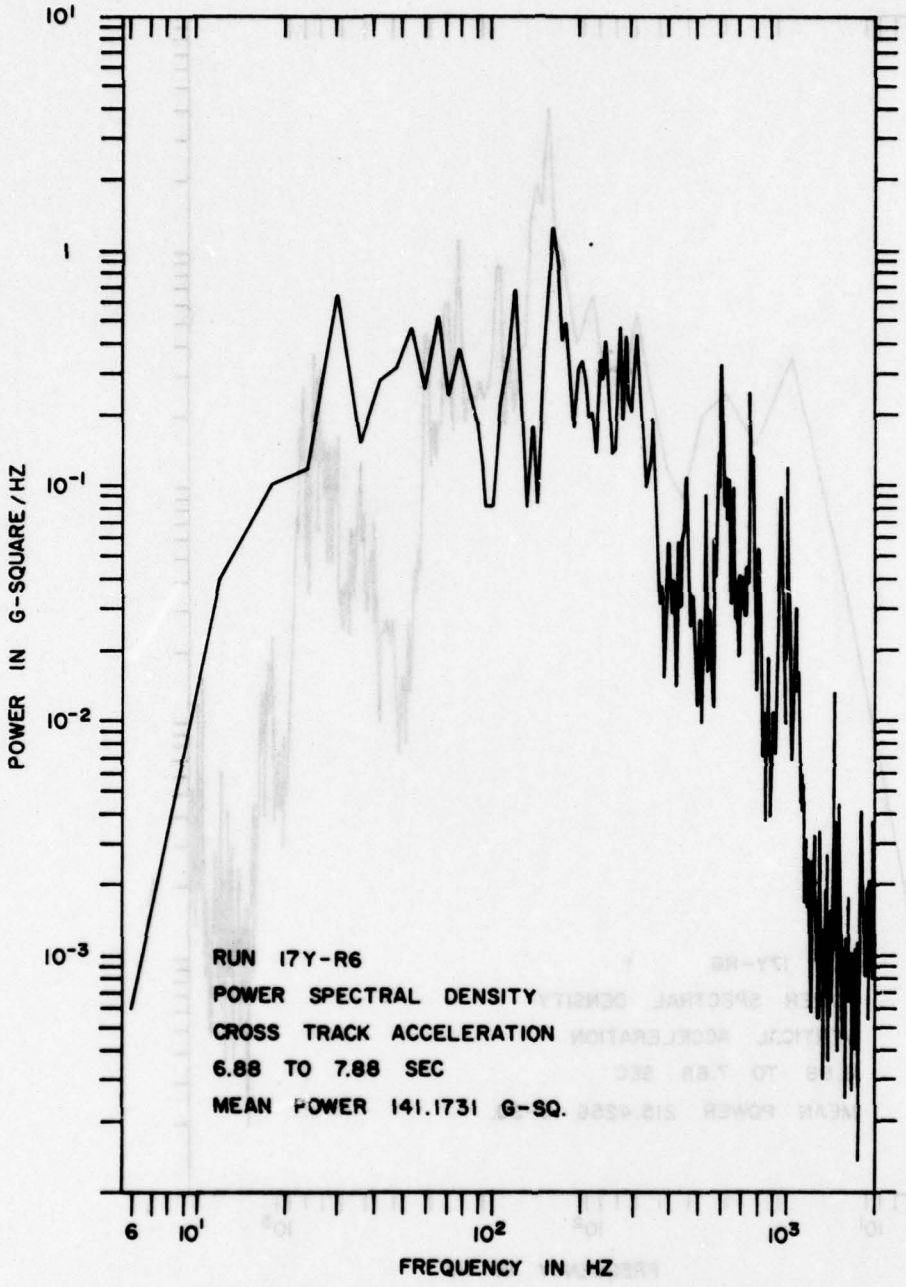

FIGURE 12. SLED/MODEL INTERFACE LATERAL POWER SPECTRAL DENSITY PLOT

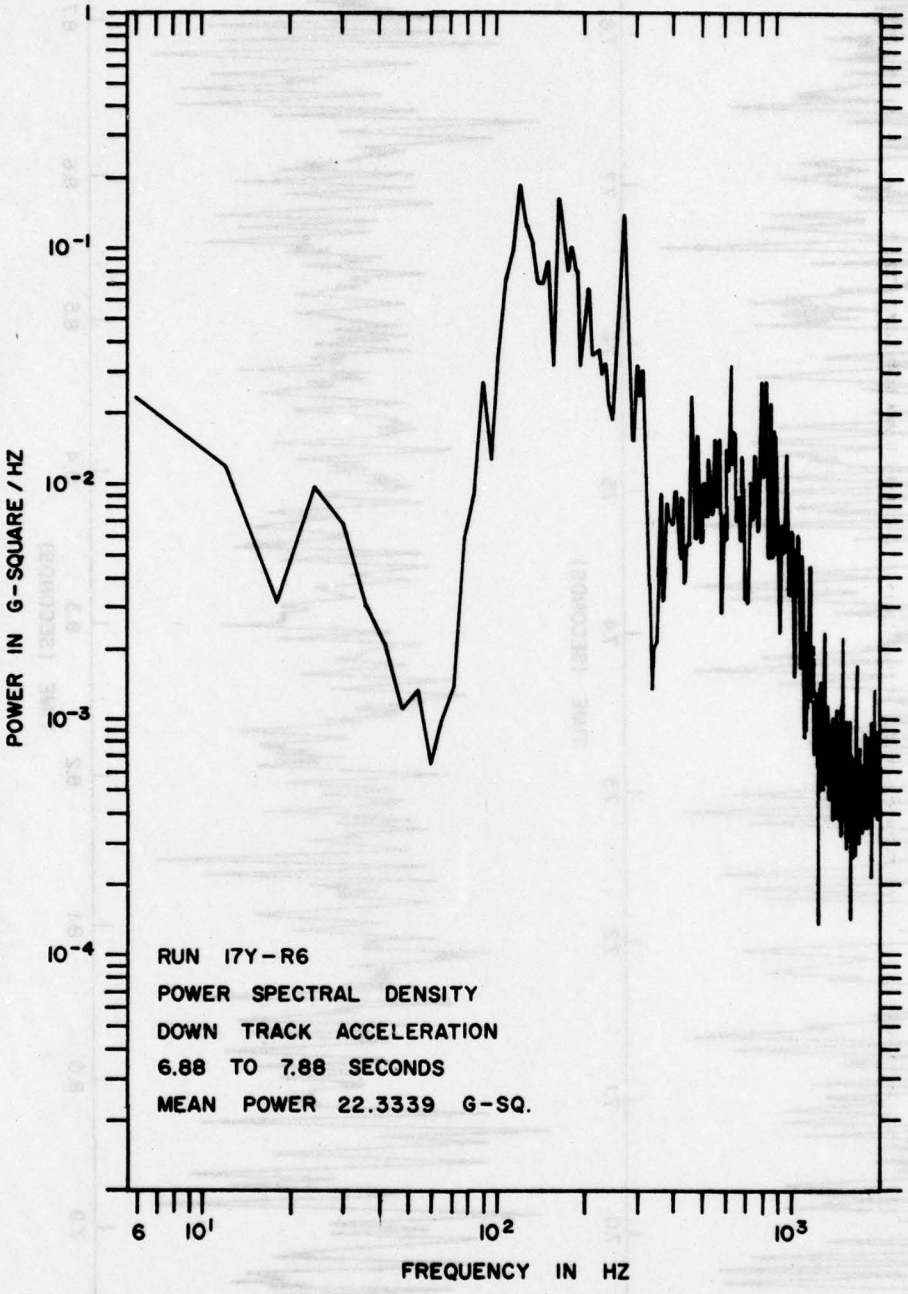

FIGURE 13. SLED/MODEL INTERFACE LONGITUDINAL POWER SPECTRAL DENSITY PLOT

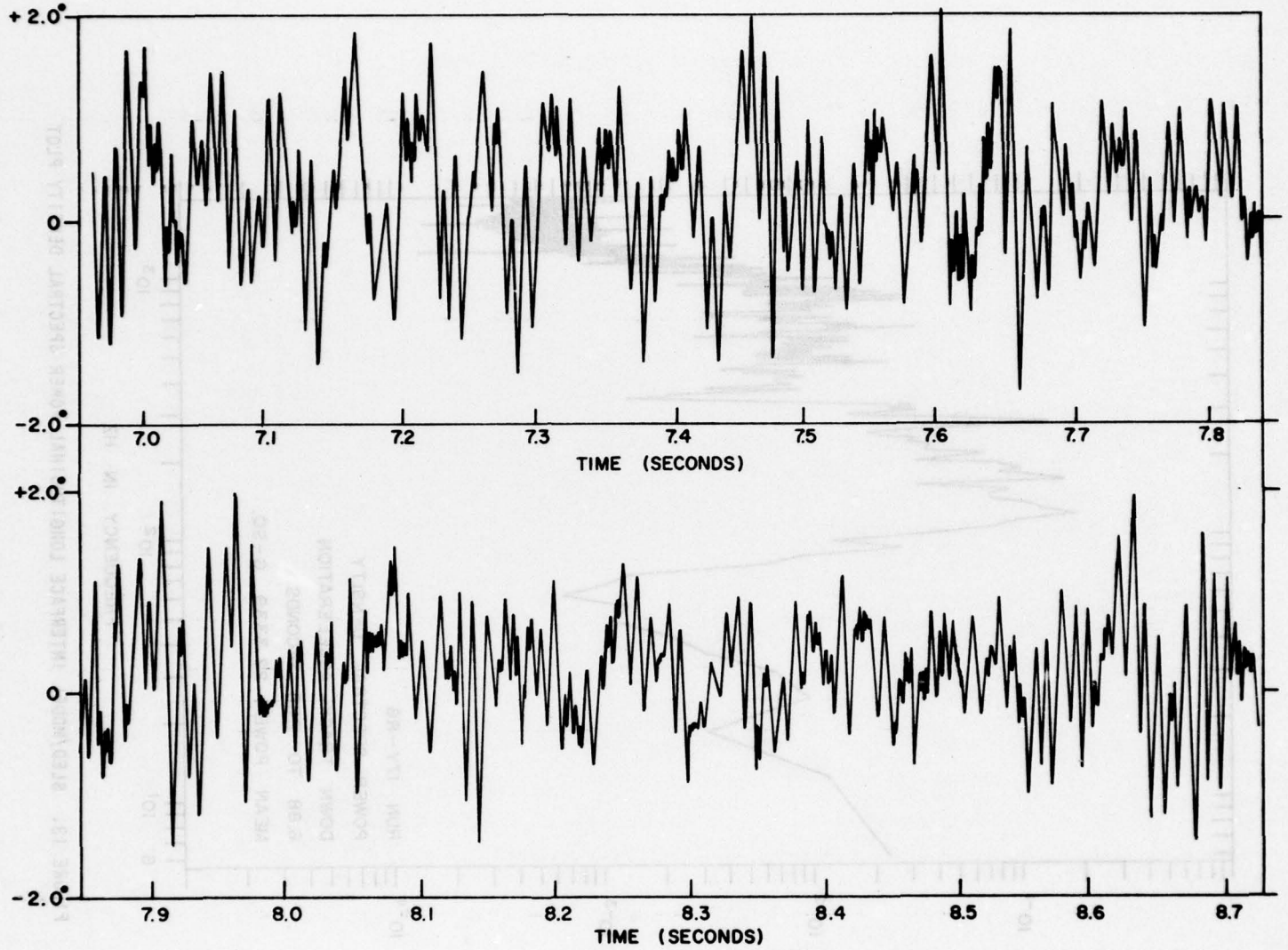

FIGURE 14. DATA SAMPLING OF MODEL AND STING DYNAMICS

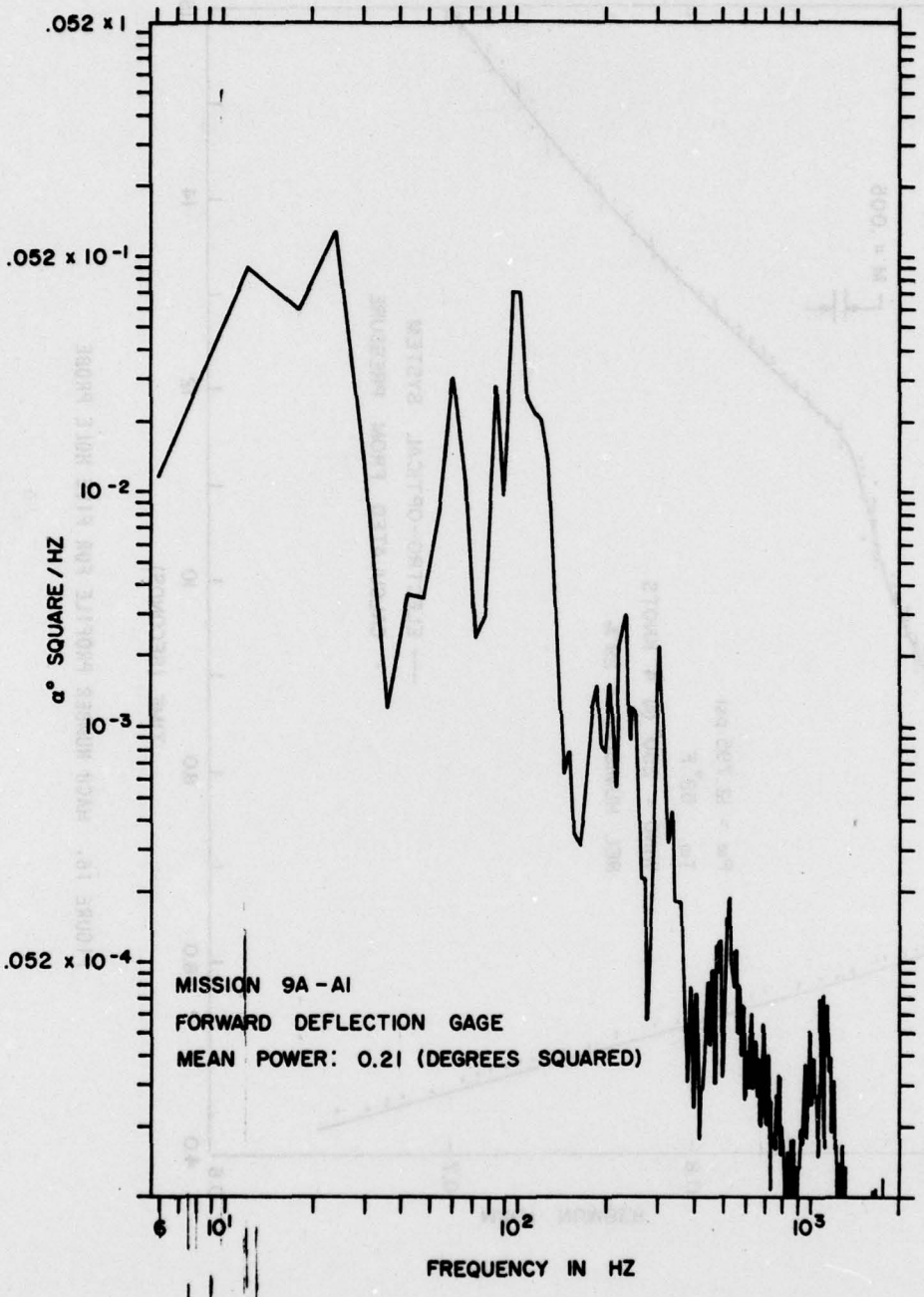

FIGURE 15. MODEL STING POWER SPECTRAL DENSITY PLOT

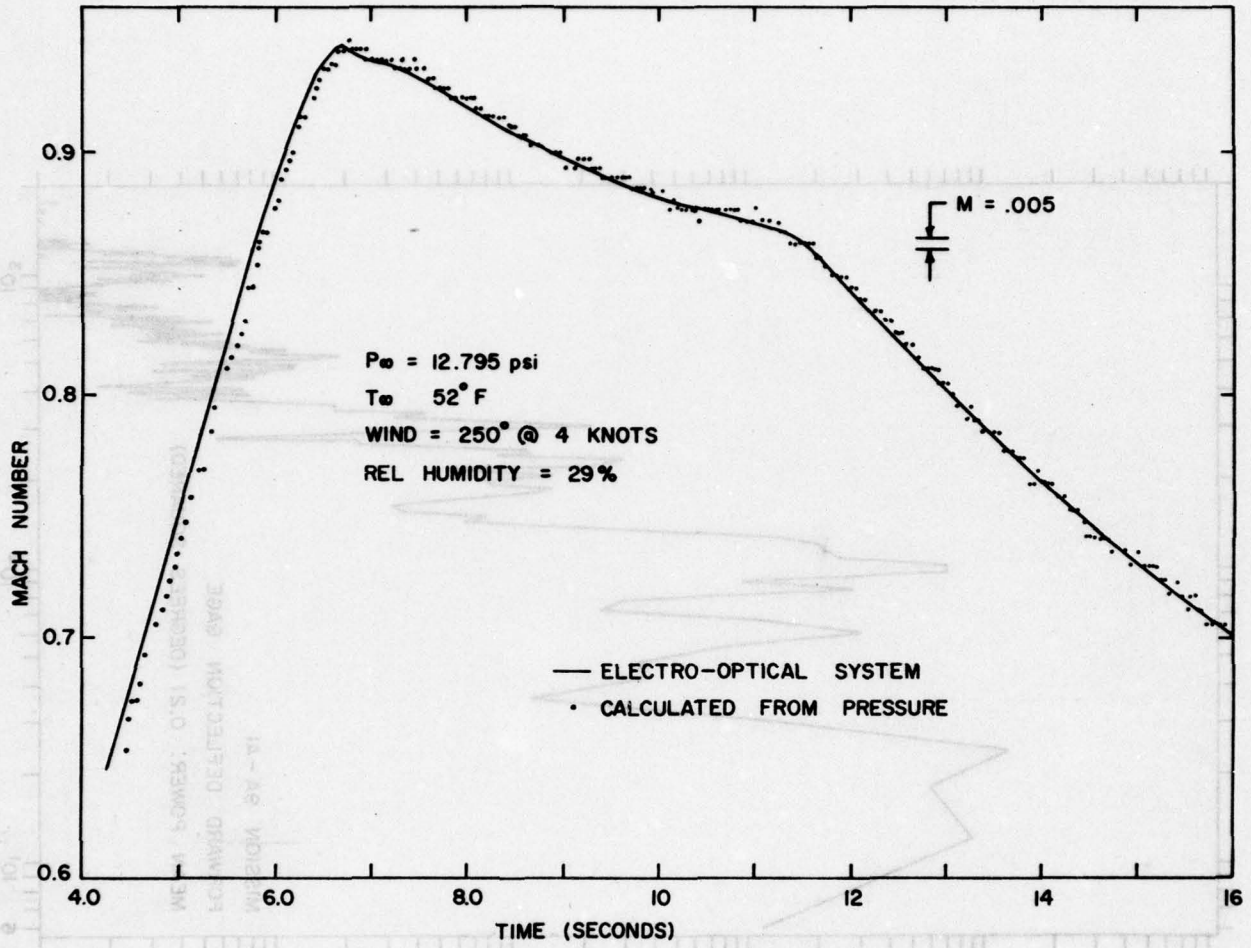

FIGURE 16. MACH NUMBER PROFILE FOR FIVE HOLE PROBE

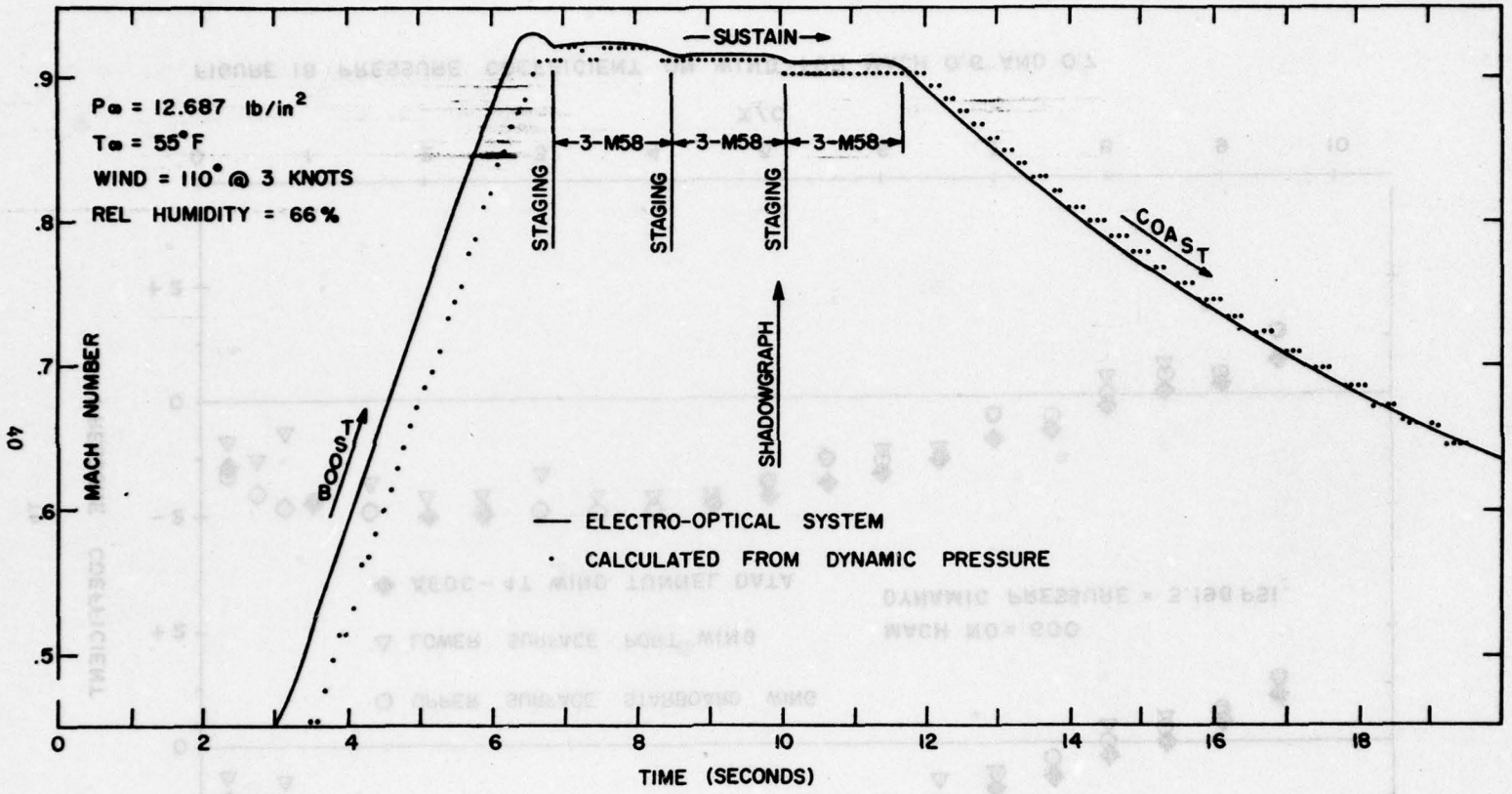

FIGURE 17. MACH NUMBER PROFILE FOR FLOW SURVEY MODEL (RUN 9A-1)

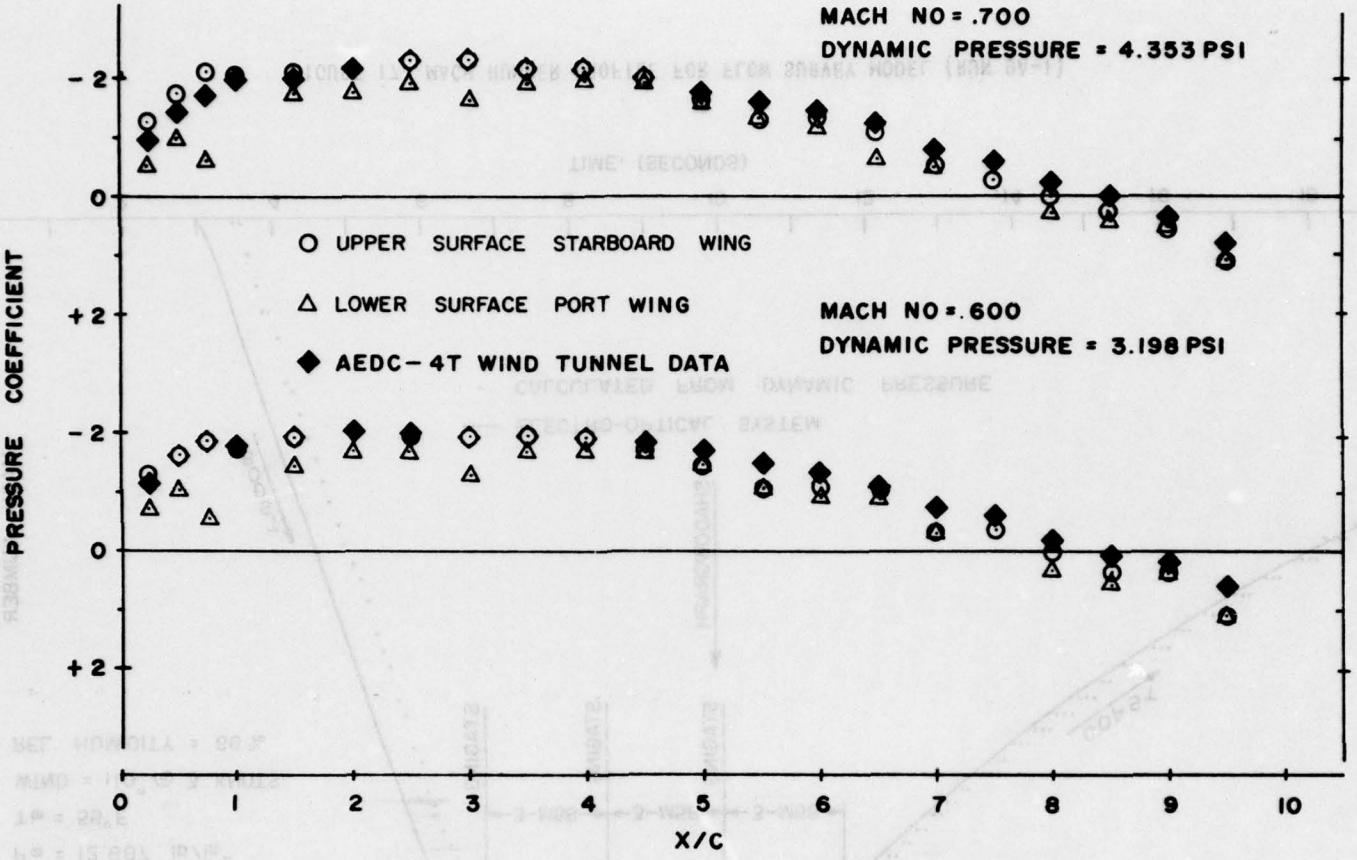

FIGURE 18 PRESSURE COEFFICIENT ON WING FOR MACH 0.6 AND 0.7

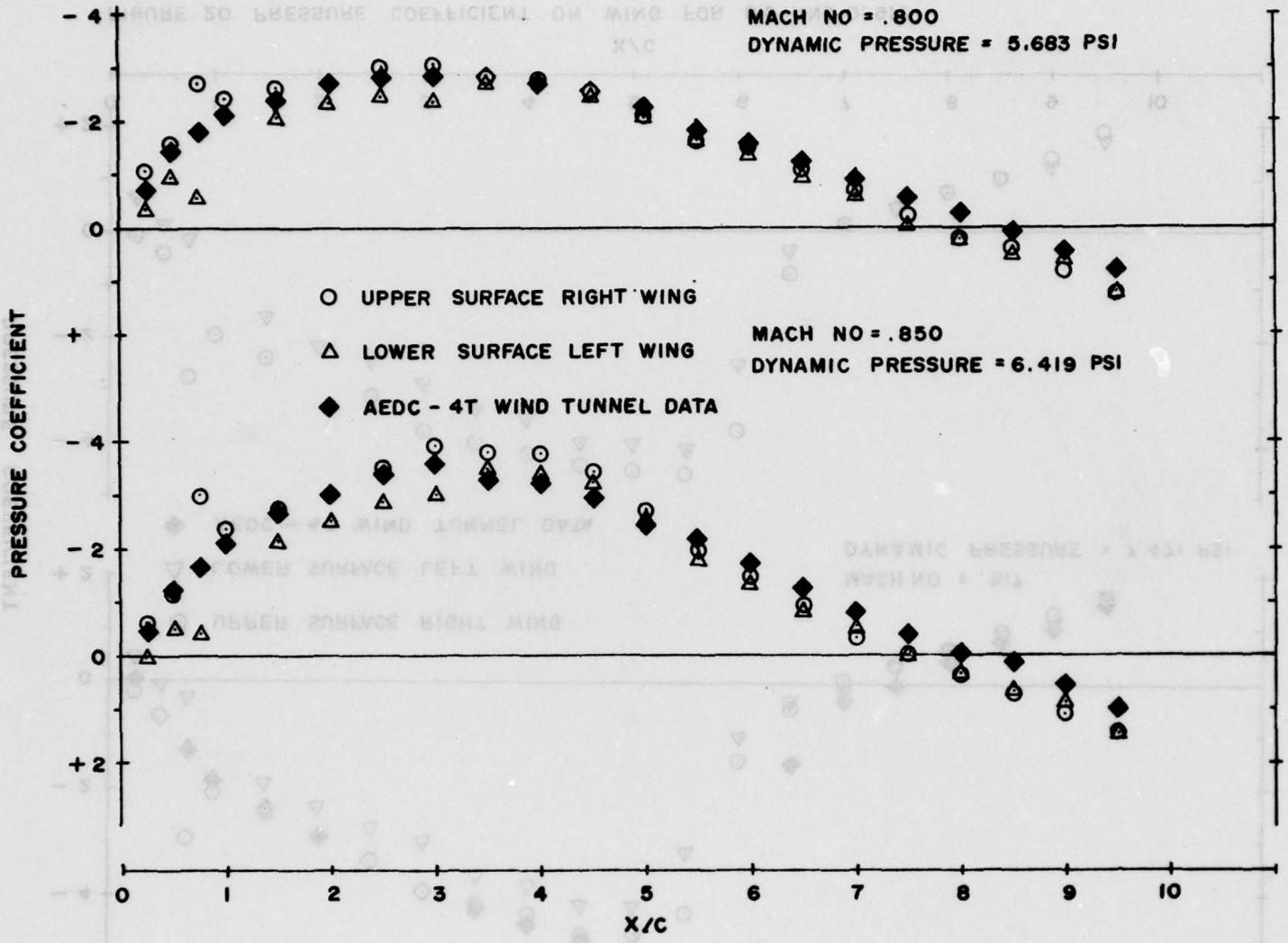

FIGURE 19 PRESSURE COEFFICIENT ON WING FOR MACH 0.8 AND 0.85

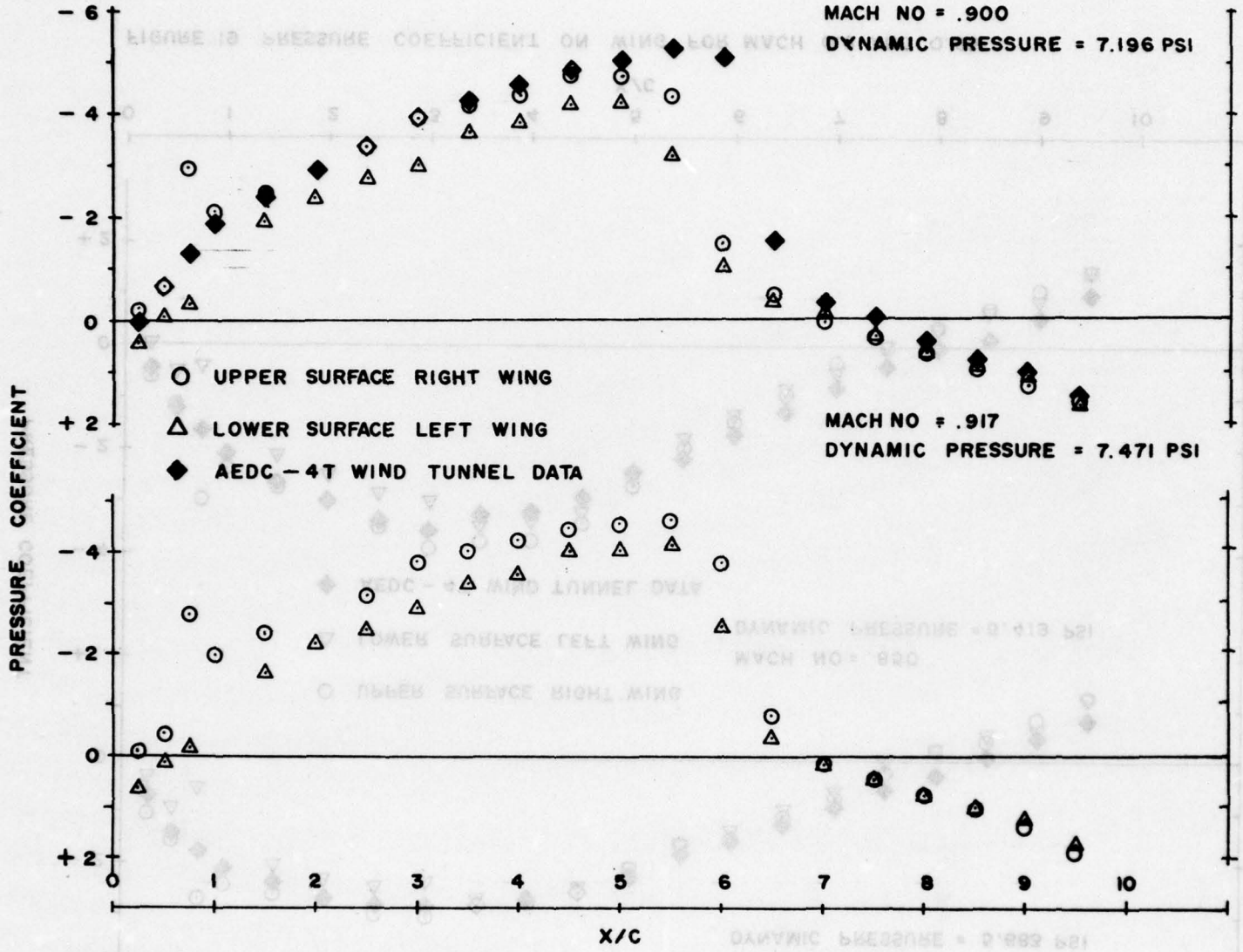

FIGURE 20 PRESSURE COEFFICIENT ON WING FOR 0.9 AND 0. 917

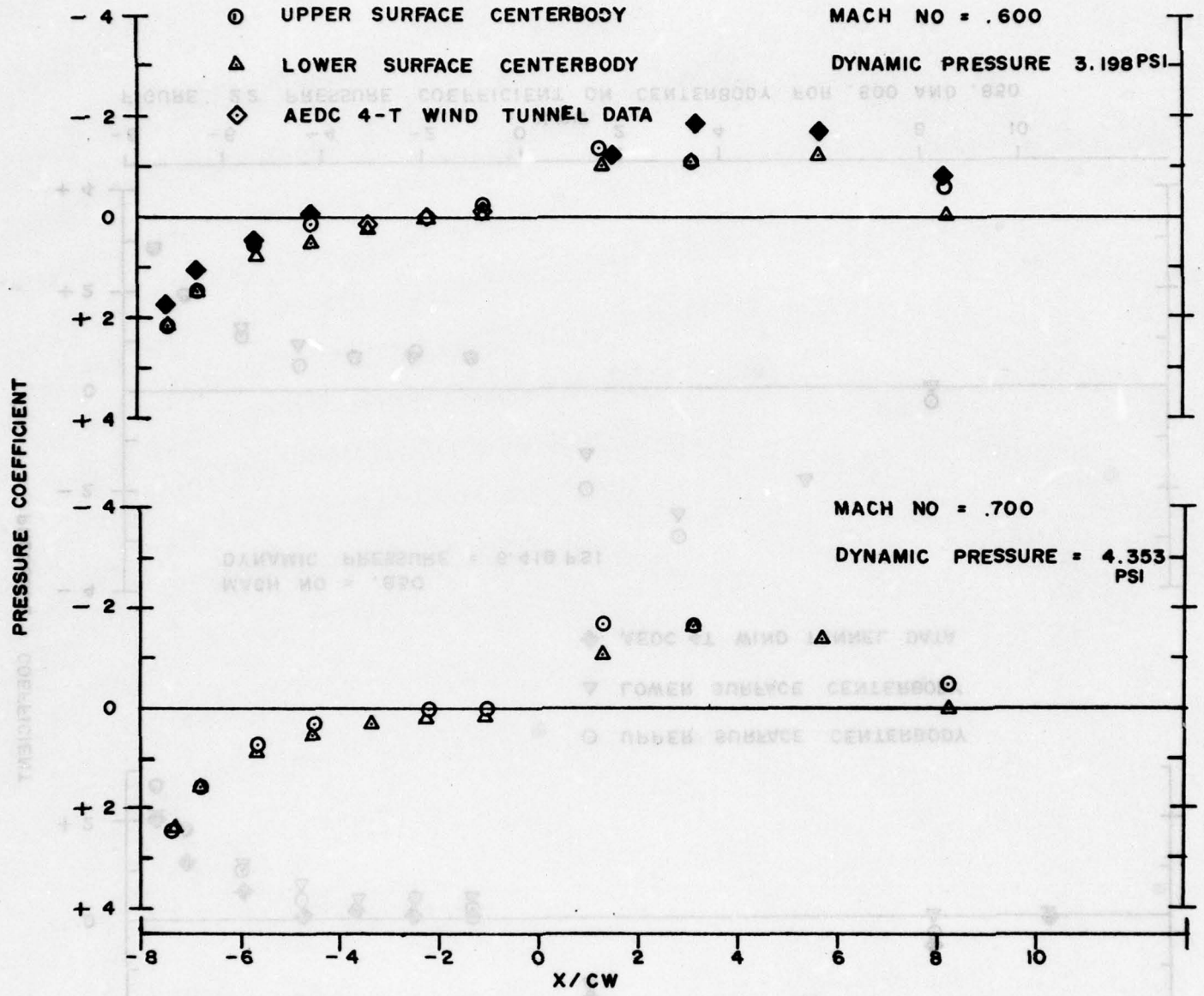

FIGURE 21 PRESSURE COEFFICIENT ON CENTERBODY FOR MACH .6 AND .7

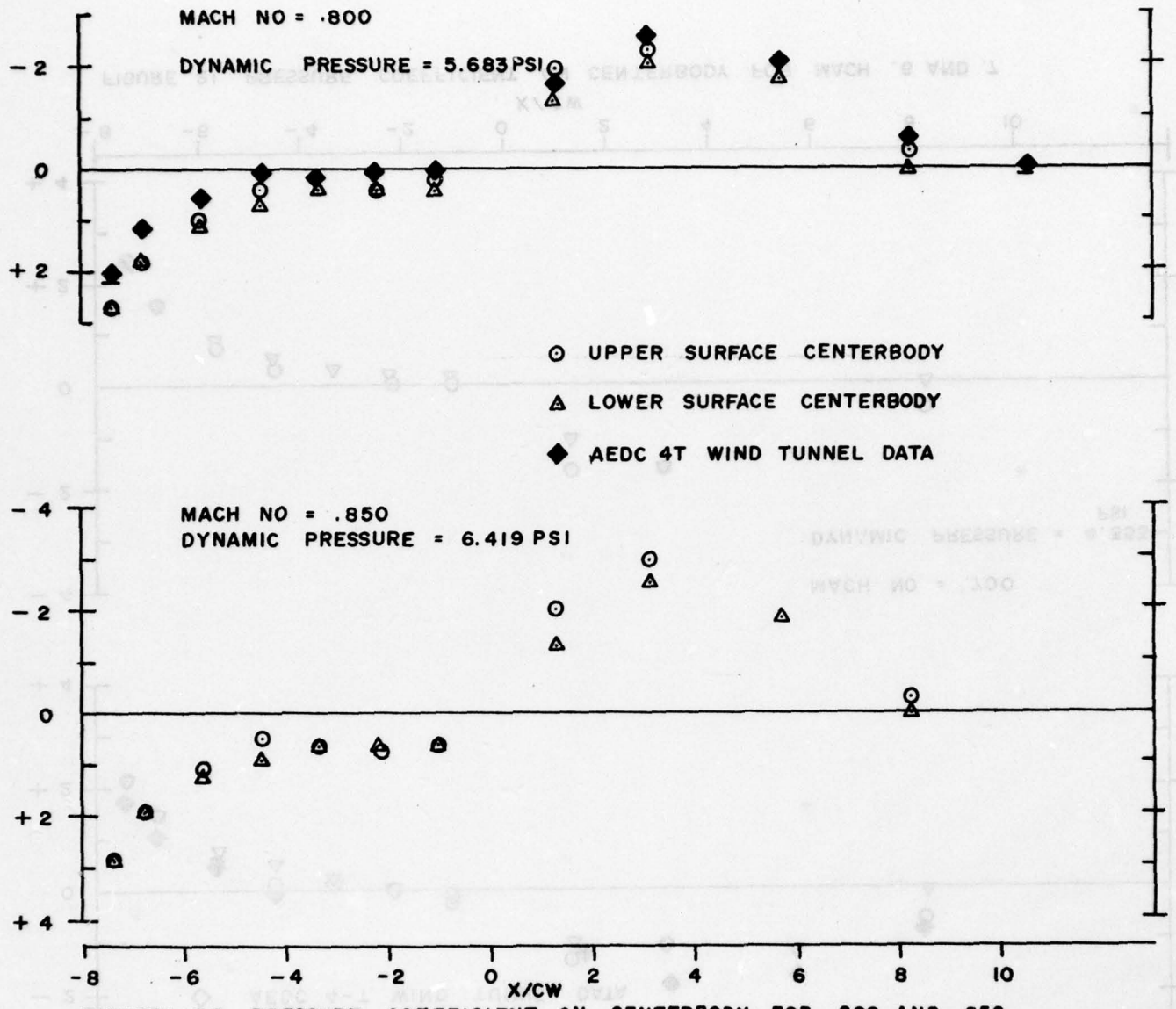

FIGURE: 22 PRESSURE COEFFICIENT ON CENTERBODY FOR .800 AND .850

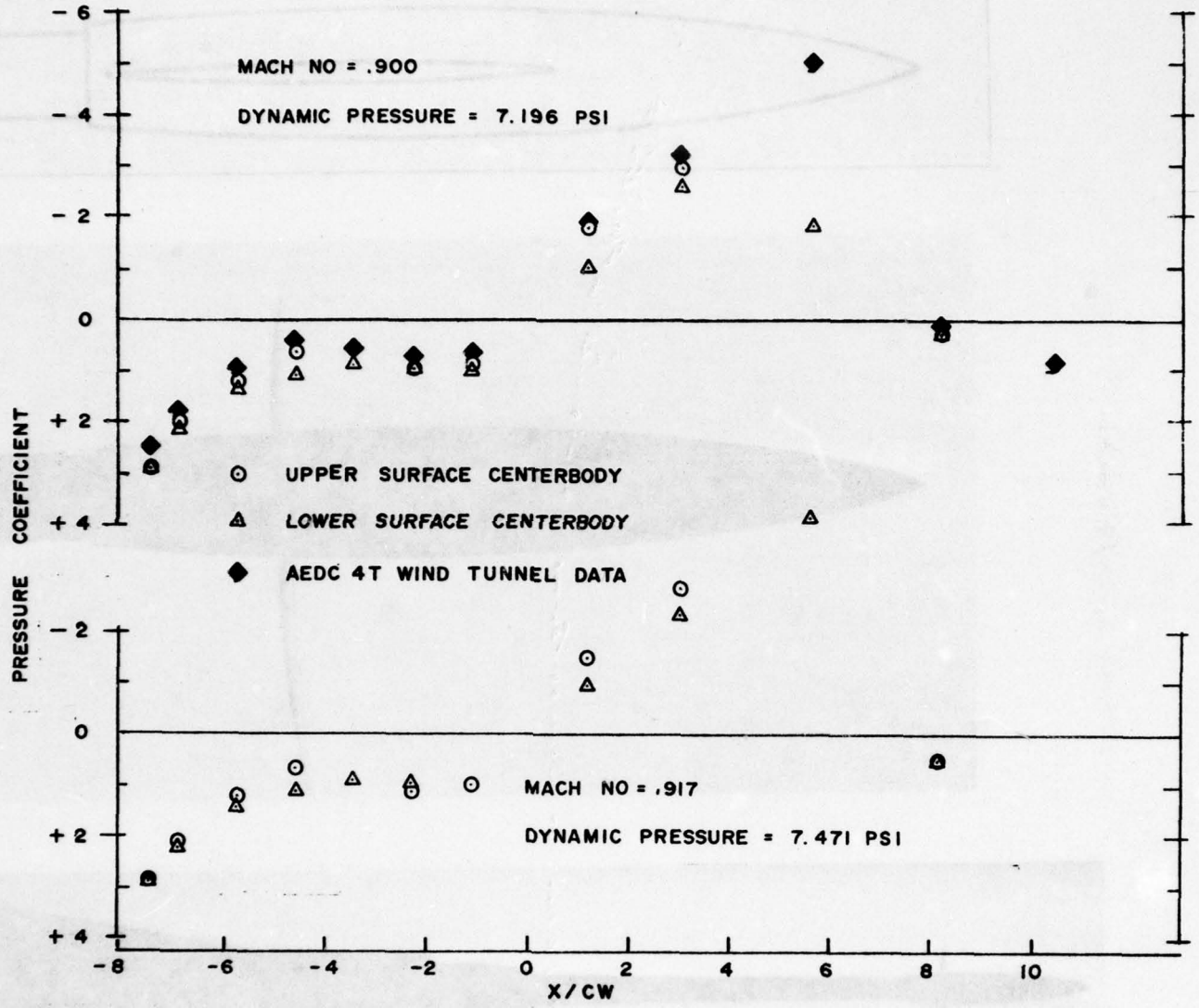

FIGURE 23 PRESSURE COEFFICIENT ON CENTERBODY FOR 0.9 AND 0.917

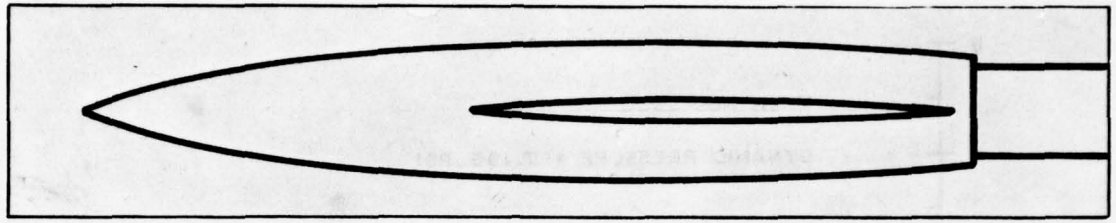

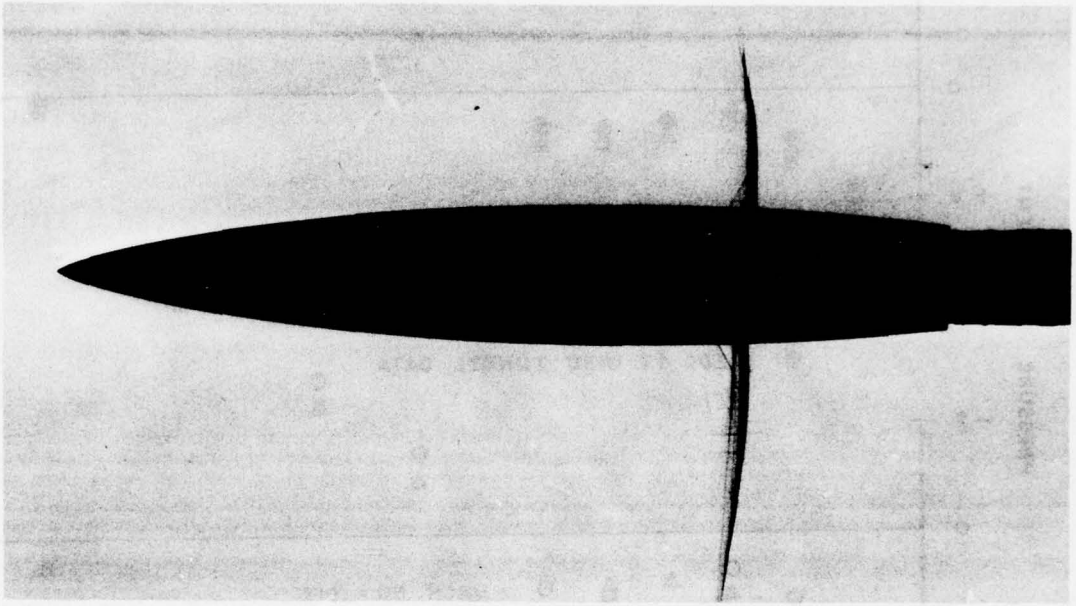

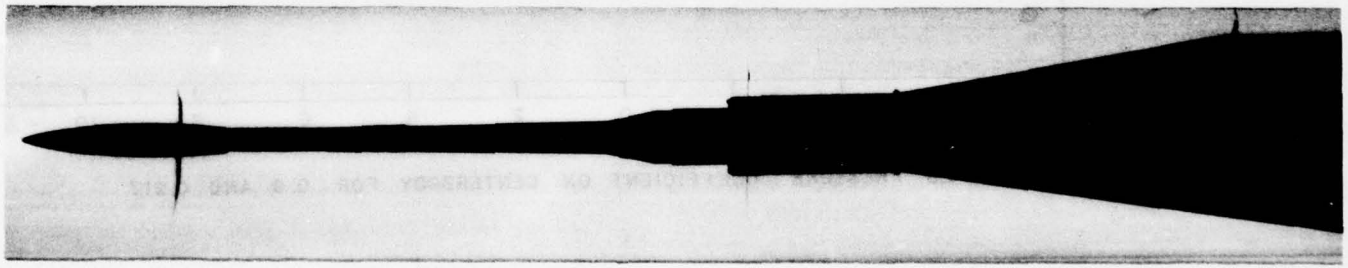

FIGURE 24. SHADOWGRAPH OF FLOW SURVEY MODEL AT MACH = 0.917

DISTRIBUTION LIST

Organization	Number Copies
DDC/TIAAS Cameron Station Alexandria, VA 22314	12
ADTC/DLOSL Eglin AFB FL 32542	1
ADTC/TE Eglin AFB FL 32542	1
3201ABG/HO Eglin AFB FL 32542	1
AU Maxwell AFB AL 31142	1
NASA Ames Research Center Moffett Field CA 94305	2
DY (R. O. Dietz) Arnold Engineering Development Center Arnold Air Force Station TN 37389	2
AFFDL (Dr. Zonars) Wright Patterson AFB OH 45433	2
6585TESTG Holloman AFB NM 88330	
TSL	2
CC	1
XR	1
GD	1
TK	1
TKI	2
TKE	3
TKS	2
TKO	5

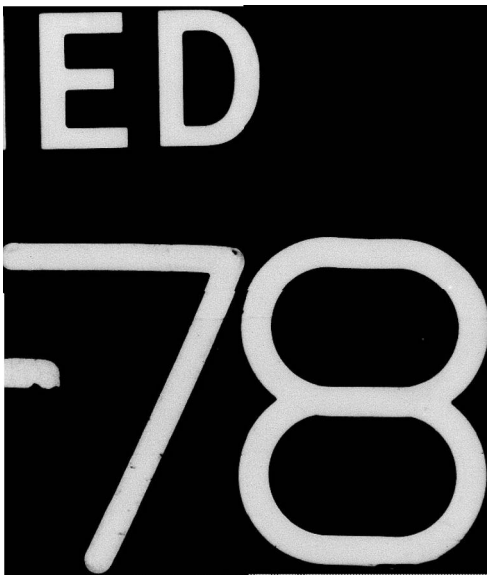
ED
78